Final Report

Effects of Thermal Mass on Heat Transfer through Wall, Cooling Load and Energy Consumption of Air-Conditioner

Dr.Pattana Rakkwamsuk
School of Energy, Environment and Materials
King Mongkut's University of Technology Thonburi

This research project is fully granted by
National Research Council of Thailand
Fiscal year: 2552 B.E.

ABSTRACT

Thermal mass of building envelope has a significant effect on the cooling loads of a building and energy consumption of an air-conditioning system. It reduces and delays peak cooling loads, and, in some cases, improves thermal comfort inside buildings. This study investigated the effects of the thermal mass of the building envelope under different conditions at orientation, various times of use in a building, and different window to wall ratios (*WWR*). The study consists of 3 parts. Part 1 is an investigation of the appropriate thermal mass on opaque wall. Part 2 is an investigation of the effects of thermal mass under different *WWR*. Part 3 is an evaluation of the insulation position of the massive wall. The annual cooling coil load from heat conducting through the wall is a main criterion for evaluating the optimal thermal mass.

'BESim', a building energy simulation tool, was employed for the study. However, a series of experiments were conducted to calibrate and validate BESim. It was found that the simulated results correspond closely with the measured heat flux surface, results the inner surface of the building envelope. The root mean square error and the mean bias error were found to be 2.547 W/m^2 for and +1.881 W/m^2 , respectively.

Heat transfer through the building envelope is subject to the thermal mass quantity, orientation and the operating time of an air conditioner. For opaque walls, the thermal mass from 200 kJ/m^2K to 300 kJ/m^2K is suitable for buildings used during the daytime and 24 hours, while a wall with low thermal mass is suitable for a building that is used in the evening and at night. *WWR* of a building envelope also has an influence on the heat stored in the building structure. As increasing the value of *WWR*, solar radiation penetrating through a window is dominant when compared to the heat conducted through thermal mass. It was found that the effect of thermal mass diminishes as WWR increases.

The study on the effect of insulation position on the cooling loads reveals that the influence of insulation is reduced when increased *WWR*, and, the position of the insulation has a small effect on the reduction of the annual cooling coil load, for a building with a massive wall and one that is used at night. It was also found that the inner mass on the insulated wall affects the high cooling coil load at night, due to the heat that was stored and trapped inside the wall.

Keywords: thermal mass , building envelope, operation time, *WWR*, cooling coil load

CONTENTS

LIST OF TABLES

LIST OF FIGURES AND DIAGRAMS

LIST OF SYMBOLS AND ABBREVIATIONS

ρ = material density (kg/m^3)

c_p = specific heat (J/kgK)

WWR = window to wall ratio

BESim = Building Energy Simulation program

α = thermal diffusivity (m^2/s)

k = thermal conductivity (W/mK)

Δx = thickness (m)

ΔT = temperature difference (K)

U = the overall heat transfer coefficient (kW/(m^{2}K)

A = the heat transfer area (m^2)

m = mass (kg)

T_a = the ambient temperature (^{o}C)

T_i = the inside temperature (^{o}C)

q = heat flux (W/m^2)

ε_{wor} = emittance of thermal radiation of the outer wall surface

σ = stefan-Bolzmann constant

α_{wor} = absorptance of thermal radiation of the outer wall surface

ε_{sky} = emittance of the equivalent sky surface

T_{sky} = equivalent absolute temperature of the sky (K)

ε_g = emittance of ground,

T_{sky} = absolute temperature of ground (K)

F_{sj} = view factor of the wall to the j th surface in front of the plane above ground level

J_{sj} = radiosity or total radiation out from the j th surface, above ground

F_{gj} = view factor of the wall to the j th surface at ground level

J_{gj} = the radiosity of the j th surface at ground level

h = heat transfer coefficient (W/m^{2}K)

CHAPTER 1
INTRODUCTION

1.1. Rationale

As a result of the looming shortage of fossil fuel reserves in the earth and the disastrous climate change caused by global warming, many countries are striving to enhance energy efficiency, and to promote renewable energies in the building sector. Existing buildings are responsible for over 40% of the world's total primary energy consumption, and account for 24% of world CO_2 emission (IEA, 2006). Energy consumption in building is allocated for satisfying the buildings' energy needs for heating, cooling, lighting and the other electrical appliances and equipment. A number of countries in the world have adopted mandatory requirements on energy conservation for building (K.B. Janda *et al*, 1994). Any strategic plans to promote energy efficiency and energy conservation in buildings, would exert a significant impact on the reduction of the energy use in the country as a whole.

The maintenance of indoor comfort in modern buildings is usually ensured by air conditioners, particularly in a hot climate. 70.9 % of all the electricity used in urban households in Thailand is consumed by air conditioner (Chirarattananon, 2005). The impact of the use of air conditioners on electricity demand is a serious problem. Peak electricity loads force utilities to build additional power plants, in order to satisfy the demand, thus increasing the average cost of electricity. In order to reduce the cooling load of air conditioners, we need to prevent occurring heat gains in building.

The amount of heat accumulated in a building depends on many factors. The prominent factors are the heat capacity of the structure, schedule of use of space (and air-conditioning), and ambient conditions (Saman *et al*, 1991). The design and construction of the envelope of building, can have a significant effect on the building's comfort and energy consumption. A breakdown of the cooling load of a typical office building in Thailand, shows that heat gain through the building envelope is dominant, at almost 60% of total. Electric lighting is the second largest user, at around 20% of the total (Chirarattananon, 2005). The envelope and the air conditioning system are closely interrelated, and the proper management of the thermal capacity can influence very drastically the power requirements for heating and air conditioning (Fernandez *et al*, 2005).

A crucial factor that influences the heat capacity of the building envelope is thermal mass. Thermal mass, which is a function of material density (ρ) and specific heat (c_p), is a measure of the heat storage capacity of the material (Gregory *et al*, 2007). When exposed to external heating, the thermal mass absorbs and stores the solar heat gain during the day, and then slowly releases it into the inside environment later on. For centuries, the vast majority of European and Middle Eastern residential buildings have been built using massive walls (Kosny *et al*, 2000). Effective use of structural mass for thermal storage has been shown in several studies. It reduces building energy consumption, reduces and delays peak heating and cooling loads, and, in some case, improves comfort (Balaras, 1995, Kosny *et al*, 2000 and Kalogirou *et al*, 2001).

Solar radiation is the main driving force promoting heat gain through the building envelope (Chirarattananon, 2005). The amount of total solar radiation on the building surfaces is related to location, time and the orientation of that building. Thus, the cooling load is related to the quantities of thermal mass and the building operating time. Moreover, solar heat can enter into buildings, by being conducted through building materials and entering through transparent openings (Balaras, 1997), and thermal mass can also absorb heat from inside building. Thus, window area also influences the effectiveness of thermal mass and it should be considered in building design as well. There are several studies (Gregory *et al*, 2007, Fernandez *et al*, 2005, Ogoli, 2003, Kosny *et al*, 2000, Givoni, 1998 and Argiriou, 1992) regarding the effectiveness of thermal mass for reducing energy consumption in buildings. However, they have not quantified the suitable thermal mass for different operation times in air-conditioned buildings and they have not considered the influence of window area on the effectiveness of thermal mass.

Thailand is located in a hot humid tropical zone, where the main electricity in residential buildings and commercial buildings is consumed by air conditioning loads. A reduction of electricity consumption by the air conditioning systems, by means of suitable design on the thermal mass of building envelopes should be of interest.

This study presents the results of several simulations, which investigate the thermal mass effects of building envelopes under different orientations, various time uses of buildings, and different *WWR*.

1.2 Objectives

1. To investigate the thermal mass affecting air conditioned building envelopes, in terms of annual cooling coil loads in cardinal directions (north, south, east and west), and to look at the differences in building operation times.
2. To investigate the thermal mass effects of the difference of window to wall ratio (*WWR*).
3. To evaluate the effect of the position of insulation and thermal mass in massive walls, to reduce the cooling load in buildings.

1.3 Scope of the Research Work

- The case of parameterization studies is constructed, by using a simulation model, Building Energy Simulation (BESim), based on Thailand weather data, developed by V.D. Hien (2000).
- For simulation, only the heat transfer through the wall has to be taken into account.
- The accuracy of the simulation program is verified by actual field experiments.

CHAPTER 2
LITERATURE REVIEW & THEORIES

2.1 Review of the Role of Thermal Mass

The term thermal mass is commonly used to signify the ability of materials to store significant amounts of thermal energy and delay heat transfer through a building component (Kalogirou *et al*, 2002). The storage material, which is referred to as thermal mass, is the construction mass of the building itself (Balaras, 1996). Components of thermal capacitance of the envelope and the interior mass, quantify the ability of the building to store thermal energy (Antonopoulos *et al*, 1999).

2.1.1 Parameters in Term of Thermal Mass

In previous studies, the thermal mass or heat storage capacity was determined in the different terms of parameters. Balaras (1996) has included parameters for describing thermal effects from several studies, as shown in Table 2.1.

Kalogirou *et al* (2002) characterized thermal mass by the thermal diffusivity α of the building material, which is defined as $\alpha = k/(\rho C_p)$, where k is thermal conductivity of the material, W/(mK), ρ is density of the material, kg/m^3, C_p is the specific heat of the material, J/kgK. Heat transfer through a material with high thermal diffusivity is rapid, the amount of heat stored in it is relatively small, and the material responds quickly to changes in temperature.

Antonopoulos *et al* (1999) and Kontoleon *et al* (2007) introduced thermal capacitance of building, by adding the distributed specific heats of all building into a lumped capacitance, i.e.

$$C_a = \sum v_j \rho_j c_j$$

where v_j, ρ_j, c_j are the volume, density and specific heat, respectively, of the concrete frame, exterior and interior wall layers, floor and roof layers, fenestration, furniture, etc..

For the this study, thermal mass is defined, according to the standards of energy conservation in buildings drawn up by the Department of Alternative Energy Development and Efficiency, DEDE, Thailand. The thermal mass is represented by the product of the density ρ *(kg/m^3)* and the specific heat C_p *(J/kgK)*, multiplied by the thickness Δx *(m)* of materials,

$$\text{Thermal mass} = \rho C_p \Delta x \quad (J/m^2K) \text{ (DEDE, 2007).} \qquad (2.1)$$

Table 2.1 Parameters for describing thermal mass effects (Balaras, 1996).

Parameters	Physical meaning	Ref.
Admittance factor	Represents the extent to which heat enters the surface of materials in a 24-hour cycle of temperature variation	Burberry,1983
Capacitance	Accounts for the ability of the external and internal materials to store heat	Shaviv *et al*, 1978
Comprehensive transfer functions	Describes heat flows in building elements, combining individual wall transfer functions for and enclosure	Seem *et al*, 1998
Conduction transfer functions	Expresses the decay of temperature through the material	Kusuda,1985
Cooling load temperature difference	Includes the effect of time lag in the propagation of heat through the material, due to thermal storage	Antinucci, 1990
Diurnal heat capacity	Measures the effectiveness of thermal material for heat storage during a continuous 24-hour cycle	Bacomb *et al*, 1988
Effective heat capacity	Accounts for the effects of the building materials' thermal properties and design factors on the long-term energy performance	Givoni, 1987
Effective heat storage	accounts for the effects of thermal capacity and thermal resistance of the building elements, and the exterior resistance, for exterior and interior building elements	Mathews *et al*, 1989
Effective thermal capacity	Accounts for the effective mass of the building elements	Mathews *et al*, 1991
Envelope heat transfer coefficient	Includes the effects of thermal transmittance of the material along with heat transfer rate due to infiltration	Burch, 1984
Heat capacity	Introduces the effect of heat storage for different building types in the correlation coefficients used in calculating the solar saving fraction	Givoni, 1987
Mass effect coefficient	Accounts for the temperature fluctuation allowable in the space, the amount of heat gain due to ambient conditions, and the degree of exposure of the space to ambient conditions	Bida *et al*, 1987
M-factor	Corrects steady state U-values for the building materials	Catani,1978
Solar saving fraction	Correlation coefficients as a function of the heat capacity for specific building types	Givoni, 1987
Thermal capacity	Determines the heat flow in unit time by conduction through unit thickness of a unit area material, across a unit temperature gradient, defined as the product of density by specific heat	Mass *et al*, 1991
Total thermal time constant	The heat stored in a whole enclosure per unit of heat transmitted to or from the outside through the elements surrounding the enclosure and by ventilation	Givoni, 1981

2.1.2 The Phenomenon of Heat Transfer in Building Envelopes

Balaras (1996) described the temperature distribution and heat transfer in a building element, by using Fig.2.1. Initially, the building element is at thermal equilibrium. As time progresses, the outside surface temperature of the element increases and, owing to the temperature difference within the element, heat is transferred from the outside to inside. The temperature of the element increases, with higher temperatures closer to the outside surface. At noon, the outside temperature reaches a maximum value, and from there on it decreases, as the incident solar radiation also decreases. As a result of the material's thermal inertia, interior locations inside the building element retain higher temperatures. As time progresses, the heat wave is transferred to the tight, towards lower temperatures. A similar cycle follows the next day.

Indoor conditions are directly linked to prevailing outdoor conditions. This results in temperature swings, with peaks occurring during the most unfavourable periods of the day, around noon and early afternoon. During these periods of the day, high outdoor temperatures eliminate the use of simple alternative passive cooling techniques, such as natural ventilation. Consequently, in order to maintain thermal comfort during these hours, it is necessary to remove all excess heat from the space immediately upon entry, with an energy-consuming mechanical system. This will require an oversized system, capable of handling the short-period peaks of the cooling load.

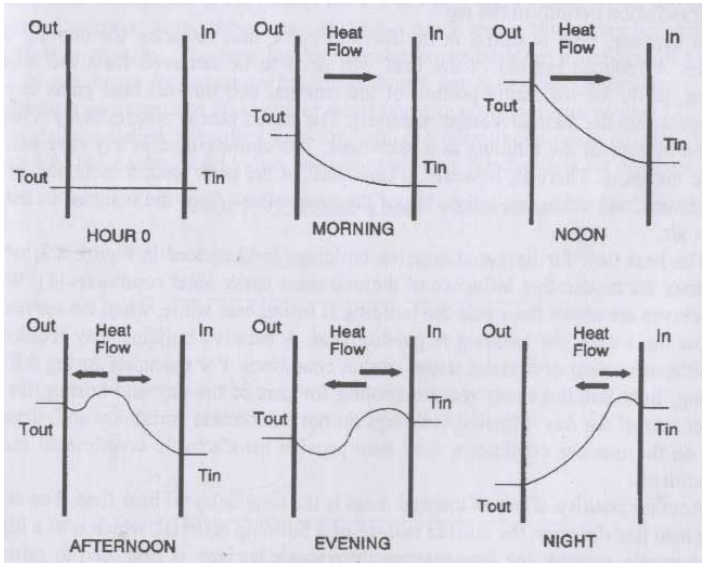

Fig.2.1 Diurnal temperature distribution and the heat transfer mechanism of a building element (Balaras, 1996).

2.1.3 The Role of Thermal Mass on the Thermal Performance of buildings

To reduce indoor air temperature and cooling load peaks, and to transfer the load to a later time in the day, it is possible to store heat in the material of the outer envelope and the interior mass of the building. The delay of heat transfer through a building leads to three important results (Balaras,1996, Kosny *et al*,2000 and Kalogirou *et al*, 2002):

- the slower response time tends to moderate indoor temperature fluctuations caused by outdoor temperature swings,
- in hot or cold climates, it reduces energy consumption in comparison to that for a similar low-mass building, and
- it moves building energy demand to off-peak periods, because energy storage is controlled through correct sizing of the mass and interaction with the HVAC system.

2.2 Review on Parameters Influencing the Performance of Thermal Mass

The rate of heat transfer through building materials and the performance of thermal mass is determined by a number of parameters and conditions. To achieve the best possible results, one needs to follow some general guidelines and take appropriate actions that fall within the overall procedure of energy-efficient building. It is important to understand the relationship of these parameters to the performance of thermal mass, in order to achieve the best possible results. Optimization of thermal mass levels depends on building-material properties, building orientation for the location and distribution, thermal insulation, ventilation, climatic conditions and use of an auxiliary cooling system, and occupancy patterns. The most important features were analyzed by Balaras (1996) in the following discussion.

2.2.1 Material Thermal Properties and Performance

The temperature distribution within the building materials varies with time, boundary conditions and material thermal properties. The phenomena which take place during the day and night, differ significantly, depending on whether the mass material is being charged (temperature increase) or discharged (temperature decrease). The thermophysical properties of heat storing materials can influence the performance of the system (Kalogirou

et al, 2002 and Balaras,1996). The stored heat energy is actually directly proportional to (Bansal, 1994)

- the specific heat capacity of the materials of the building component
- its mass
- the difference between its temperature and the surrounding temperature.

The stored thermal energy can then be calculated, by multiplying the specific heat storage with the mass of the material and the temperature difference (DEDE, 2007).

$$q = c\rho\Delta x\Delta T \qquad (2.1)$$

where c = specific heat (J/kg.K),

ρ = density (kg/m^3),

Δx = thickness of material (m),

ΔT = temperature difference (K).

For the material to effectively store heat, it must exhibit a proper density, high thermal capacity, and a high thermal conductivity value, so that heat may penetrate through all the material during the specific time of heat charging and discharging. The depth that the diurnal heat wave reaches within the storage material, depends on thermal diffusivity (the controlling transport property for transient heat transfer). Materials with higher thermal diffusivity values can be more effective for cyclic heat storage, at greater depth than materials with lower values. Beyond a certain material thickness, the heat flow into the indoor air does not take place during the night hours, but it is delayed till the following daytime hours. This is undesirable during the cooling season, since the release of stored heat to indoor spaces during the early hours of the day, will result in unpleasant indoor comfort conditions and increase early day cooling loads.

2.2.2 Thermal Mass Location and Distribution

Location of thermal mass is important. One may distinguish two cases, based on whether the heat storage material receives energy by solar radiation (direct) or by IR radiation and room air convection (indirect). Direct heat gains are experienced by the outer building envelope, which is exposed to solar radiation, and by the interior surfaces which may absorb incident solar radiation as it enters through the building's openings. Indirect heat gains are experienced by opaque elements inside the building, from the energy which

is transferred indoors from direct gain surfaces. Direct locations are much more effective than indirect, for placing heat storage mass.

Thermal mass must be properly distributed around the building, depending on the orientation of a given surface and the desirable time lag (Lechner, 1991). North and east surface orientations have little need for a time lag. For a south and west side, an 8 h time lag is sufficient to delay heat transfer from midday until the evening hours. The roof, which is exposed to solar radiation for most of the day, would have required a very heavy construction with a long time lag. However, because it is very expensive to construct massive roofs, the use of additional insulation is usually recommended instead.

2.2.3 Thermal Mass and Insulation

In general, both thermal mass and insulation are important in the overall thermal performance of a building (Hopkins *et al*, 1979). In climates where cooling is of primary concern, thermal mass can reduce energy consumption, provided that the building is unused in the evening hours, and the stored heat can be dissipated during this period. However, common insulation materials will deteriorate the performance of a thermal storage wall (Balcomb *et al*, 1988). Overall, because thermal mass stores and releases heat, it interacts with the building operation more than the simple addition of insulation (Ober *et al*, 1991). This makes analyzing thermal mass performance and the overall building thermal performance a more difficult problem to treat.

2.2.4 The Role of Ventilation

The role of thermal mass is also extended into the night period. During the summer, since outdoor night temperatures are usually lower than indoor temperatures, it is possible to cool the building by natural night ventilation. Ventilated air enhances convective heat losses from mass elements and dissipates the released heat to the lower temperature outdoor heat sink. Ceiling fans can also be used to increase indoor air movement and raise the convective heat transfer coefficient (Baer, 1983), which facilitates the process of rejecting heat from massive walls at night. The recommended night ventilation hourly rate is 90 $m^3/h\ m^2$ of the floor area (Balaras, 1996). The objective is to maximize the building thermal transmittance during the nighttime, and minimize it during daytime.

The effect of thermal mass under different ventilation, was studied by Givoni (1993). The study concluded that night ventilation had only a very small effect on the indoor

maxima of the low mass building. However, it was very effective in lowering the indoor maximum temperatures for the high mass building below the outdoor maxima, especially during 'heat wave' periods.

At the beginning of the following day, the cooled mass is utilized as a heat sink. Part of the cooling load will be passively covered by the building mass, which is at a lower temperature, provided that the building is well insulated and is not ventilated during the daytime. This means that, for air conditioned buildings, it is possible to reduce the energy consumption of the system, since it will reduce its operation time. For naturally ventilated buildings, it is possible to achieve longer periods within comfort conditions.

2.2.5 Occupancy Patterns

A designer, should keep in mind that building occupants constitute the final determining factor on the extent of utilizability of any building system, including thermal mass. Clearly, by changing the use of internal spaces and surfaces, one can drastically reduce the effectiveness of thermal storage. Consequently it is necessary to carefully consider the final use of the space, when making calculations of the cooling load, and incorporating the possible savings from thermal mass effects.

2.3 Review on the Effectiveness of Thermal Mass

Givoni (1998) monitored buildings with different mass levels in Pala, South California, under different ventilation and shading conditions. The effect of mass in lowering the daytime(maximum) indoor temperatures was evaluated. For the closed buildings with unshaded windows, the maximum temperature of the low mass building was about 2^{o}C above the high mass building. The average temperature of the low mass building above the high mass building was about 0.5^{o}C, and that above the outdoors' average was about 6^{o}C. For the closed building with shaded windows, the maximum temperature of the low mass building was about 4^{o}C above the high mass building. This means that mass is more effective in reducing the rise of the indoor temperature, caused by, heat gain through the external wall. This had greater effect than penetrating solar radiation. The shading of the windows also reduced the indoor average temperature by about 1^{o}C. From this experiment, it was seen that the patterns of the indoor maxima of the buildings correspond closely to the patterns of the outdoor average.

Kosny *et al* (2000) have presented a comparative study of the energy performance of light-weight and massive wall systems. Their experiments were performed in a wide range of U.S. climates, utilizing several building sizes and shapes. The researchers used energy performance data, which was generated by whole building energy simulations for residential buildings containing wood-framed walls. This was compared with similar data generated for four basic types of massive walls. Each wall type consisted of the same materials, concrete and insulating foam. Within the same type of walls, all sequences of materials were the same, however, individual material thicknesses changed to match necessary R-values. Massive wall R-values ranged in this work from R- 0.88 m^2K/W (5.0 hft^2F/Btu) to R-3.03 m^2K/W (17.2 hft^2F/Btu). Four basic material configurations were considered for massive walls:

- exterior thermal insulation, interior mass,
- exterior mass, interior thermal insulation,
- exterior mass, core thermal insulation, interior mass, and
- exterior thermal insulation, core mass, interior thermal insulation.

From the study, a comparative analysis of sixteen different material configurations showed that the most effective wall assembly was the wall with thermal mass (concrete), making firm contact with the interior of the building. Walls where the insulation material was concentrated on the interior side, performed much worse. Wall configurations, with the concrete wall core and insulation placed on both sides of the wall, performed slightly better, however, their performance was significantly worse than walls containing foam core and concrete shells on both sides. Potential whole building energy savings, were possible when lightweight walls are replaced by massive walls of the same R-value, were calculated for 143 m^2 one-story ranch houses located in Bakersfield, California (cooling climate). For high R-value walls, 18% of the energy could be saved for the whole building, when wood-framed walls were replaced by massive wall systems. Thermal mass layers must be in firm contact with the interior of the building in these walls. The result of the study show that energy consumption in buildings can be reduced, when light walls were replaced by massive walls, which have more heat capacity.

The role of thermal mass effects in Greek buildings has been investigated, in a study by Argiriou (1992). The thermal behaviour of two types of buildings (monozone and two-zone) was calculated for varying amounts of the buildings' thermal mass. The simulation

was carried out by using the ESP program, an official computational tool for the European Commission, developed by the Energy Simulation Research Unit, at the University of Strathclyde in Scotland.

The calculations were performed for Athens, while in total 13 different types of building materials were used. The geometry of the buildings remained the same, but the building materials changed, thus varying the effective amount of the building's thermal mass. The thermal conductivity of the materials ranged between 0.19 and 1.63 W/mK, the specific heat between 796 and 1,014 J/kgC, and the density between 600 and 2300 kg/m^3.

The cooling load was first estimated for a monozone building (5 by 5 by 3 m.), with a single window, on the south side of the building. The results of the annual cooling load per square metre of floor area, as a function of the effective thermal mass, are shown in Fig.2.2. The reduction of the cooling load is significant, up to a value of thermal mass approaching 300 kJ/m^{2}K. An additional increase beyond this value does not appear to have any significant impact on the cooling load.

For the two-zone building (15 by 8 by 3 m), the additional effects of interior thermal mass were also investigated. The building included additional windows, on all sides, as shown in Fig.2.3, although the construction materials remained the same. The results for the annual cooling load per square metre of floor area, as a function of the effective thermal mass, are also shown in Fig.2.3.

The reduction of the cooling load is again significant, up to a value of thermal mass approaching 300 kJ/m^{2}K. The absolute values of the cooling are relatively higher than the monozone building, since there are additional openings, which increase the direct solar gains and air infiltration. The thermal mass effectiveness, however, remains the same.

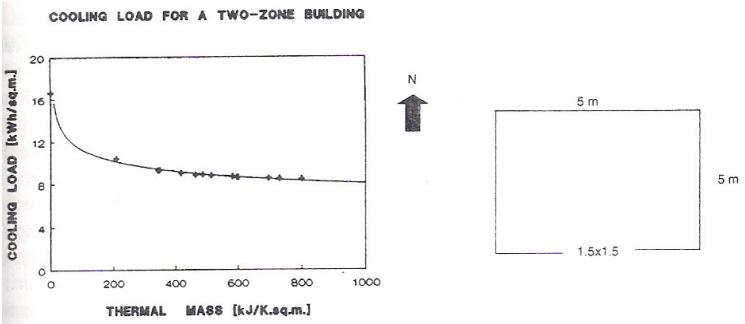

Fig.2.2 Calculated annual cooling load for different levels of thermal mass in monozone building located in Athens.

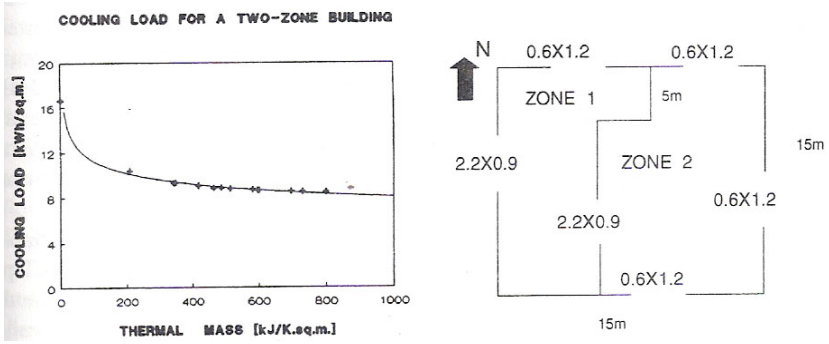

Fig.2.3 Calculated annual cooling loads for different levels of thermal mass in two-zone buildings located in Athens.

Fernandez *et al* (2005) have classified the building types, according to the effectiveness of the participation of its thermal mass, in damping extreme temperature. They proposed a lumped parameter model, for predicting the thermal response of the building, under certain weather conditions. The lumped parameter model was represented by K_t (total conductance divided by the thermal capacity) :

$$K_t = \frac{UA}{mC_p} = \frac{1}{n}\sum \frac{U_j A_j}{M_j C_j}, \qquad \text{for } 0 \le j \le n \qquad (2.2)$$

where U = the overall heat transfer coefficient (kW/(m^{2}K),

A = the heat transfer area(m^2),

m = mass (kg),

C_p = specific heat (kJ/kgK),

j = any heat transfer process of the nth set, and

n = number of heat transfer processes that occur simultaneously.

This study determined the thermal response of the building components, by considering the attenuation of the temperature variations inside the building, and a delayed effect in the inside temperature.

The attenuation was hereby expressed as the quotient of the ambient temperature amplitude ($T_{a,max} - T_{a,min}$), divided by the inside temperature amplitude ($T_{i,max} - T_{i,min}$). A very large attenuation corresponds to buildings, which are very massive. A very light building will have small values of attenuation.

The result of the study can be elaborated, as shown in Table 2.2. These results can be combined to the very simple procedure illustrated that consists in measuring the delay, and then to deciding if the building conforms to the ambient conditions.

Table 2.2 A tentative classification of building types, in terms of their thermal mass

Thermal mass	Attenuation	Delay	Building type
$1 \leq K_t^{-1} \leq 10$	Small	1-3 h	Very light
$10 \leq K_t^{-1} \leq 35$	Important	> 3 h	Comfortable
$35 \leq K_t^{-1} \leq 100$	Very effective	$\rightarrow \infty$	Very massive

Indoor temperatures in closed buildings with high thermal mass, was monitored by D.M.Ogoli (2003). It was performed in Nairobi, Kenya, which is an equatorial high altitude region. Four test chambers, each measuring 2.0m (6 ft 7 in.) long by 2.0m (6 ft 7 in.) wide and 2.0m (6 ft 7 in.) high, were built and monitored on a site in Nairobi, Kenya, during the warm period between January and March 1997. Two test chambers had timber walls, while the other two had natural stonework. Galvanized corrugated iron (GCI) sheets and concrete interlocking tiles were the roofing materials. Each test chamber was closed all the time during the experiment, but ventilation and infiltration of 0.5 air changes per hour were maintained. Peak indoor temperatures in the low mass chambers were above the peak indoor temperatures of the high mass chambers, by about 11–12 ◦C.

For indoor temperatures set at 24^{o}C, heavyweight buildings have been reported to consume less cooling energy than comparable lightweight buildings, having the equivalent thermal resistance in their walls (D.Burch *et al*, 1984). The thermal mass was also found to be more effective when it was positioned inside the wall insulation. Night time ventilation can reduce cooling loads by 27 to 36%, depending on the wall construction of the building. Larger savings occur in heavyweight compared to lightweight buildings.

2.4 Theoretical Considerations

The building wall is affected by all three heat transfer mechanisms; conduction, convection, and radiation. In general, heat may be transferred to an external surface by convection, thermal radiation, and solar radiation, which cause the surface temperature to rise. The heat is then conducted through the opaque wall and finally convected and radiated to interior space.

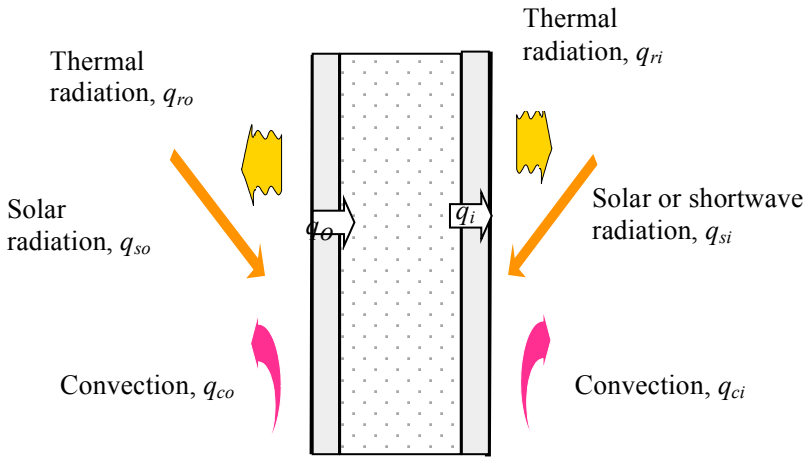

Fig.2.4 The configuration of heat transfer through opaque wall (Chirarattananon, 2005).

The analysis of energy consumption of a building must consider the heat gain through external wall, the heat transfer through building envelope and the heat transfer to the interior surface. Chirarattananon (2005) gathered information and proposed the heat balance equations, described in 2.4.1-2.4.2 .

2.4.1 Equations for the Exterior Surface of an External Wall

For the exterior surface of a wall, that faces the external environment on one side and internal environment on the other, see Figure 2.4, the net heat flux into the surface is given as ;

$$q_o = -q_{ro} + q_{so} - q_{co} \tag{2.3}$$

where q_{ro} = net thermal radiation out from the surface,

q_{so} = solar radiation absorbed at the surface, and

q_{co} = net convection heat transfer out from the surface.

For an exterior surface of an external wall with an inclination angle b , the net thermal radiation is given as;

$$q_{ro} = \varepsilon_{wor}\sigma T_{wo}^4 - \alpha_{wor}\left(\left(\frac{1+\cos\beta}{2} - \sum_{j=1}^{m} F_{sj}\right)\ \varepsilon_{sky}\sigma T_{sky}^4 + \left(\frac{1-\cos\beta}{2} - \sum_{j=1}^{n} F_{gj}\right)\ \varepsilon_g \sigma T_g^4\right)$$

$$-\alpha_{wor}\left(\sum_{j=1}^{m} F_{sj}J_{sj} + \sum_{j=1}^{n} F_{gj}J_{gj}\right) \tag{2.4}$$

where ε_{wor} = emittance of thermal radiation of the outer wall surface,

σ = stefan-Bolzmann constant,

α_{wor} = absorptance of thermal radiation of the outer wall surface,

$\frac{1+\cos\beta}{2}$ = view factor from the wall to sky,

ε_{sky} = emittance of the equivalent sky surface,

T_{sky} = equivalent absolute temperature of the sky, K

$\frac{1-\cos\beta}{2}$ = view factor from the wall to ground,

ε_g = emittance of ground,

T_{sky} = absolute temperature of ground, K

F_{sj} = view factor of the wall to the j th surface in front of the plane above ground level,

J_{sj} = radiosity or total radiation out from the j th surface, above ground,

F_{gj} = view factor of the wall to the j th surface at ground level, and

J_{gj} = is the radiosity of the j th surface at ground level.

The net solar radiation, absorbed at the surface for an opaque wall, is given as

$$q_{so} = \alpha_{wos} E_{et\theta,} \tag{2.5}$$

where α_{wos} = solar absorptance of the wall surface and

$E_{et\theta}$ = total solar radiation received.

The convection heat transfer from the surface is given as;

$$q_{co} = h_{co}\left(T_{wo} - T_o\right), \tag{2.6}$$

where h_{co} is an appropriate heat transfer coefficient.

2.4.2 Equations for Heat Transfer in a Wall

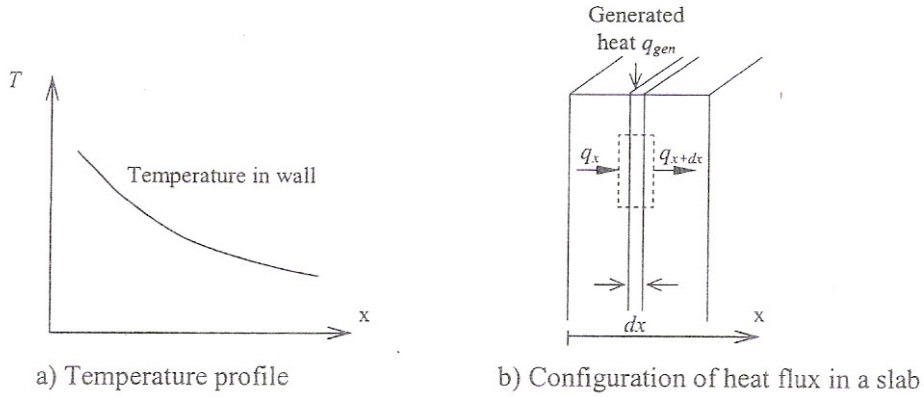

a) Temperature profile b) Configuration of heat flux in a slab

Fig.2.5 The configuration of a one-dimensional flow (Chirarattananon, 2005).

As shown in Fig.2.5, heat conduction passes through building components, at the location *x*. An equation can be written for the heat balance in a control volume, enclosed in the dotted line as follows

heat flux conducted into the volume + heat flux generated

= change in internal energy per unit area + heat flux conducted out from the volume.

This can be expressed mathematically as;

$$q_x + q_{gen} = \rho C_p \frac{\partial T}{\partial t} + q_{x+dx}.$$

It can be transformed to

$$\frac{\partial}{\partial x}\left(k \frac{\partial T}{\partial x}\right) + q_{gen} = \rho C_p \frac{\partial T}{\partial t}.$$

If *k* is not a function of x, then the equation simplifies is;

$$\frac{\partial^2 T}{\partial x^2} + \frac{q_{gen}}{k} = \frac{\rho C_p}{k} \frac{\partial T}{\partial t}, \qquad (2.7)$$

where $\alpha = k/(\rho C_p)$ is also know as thermal diffusivity of wall material.

This last equation is the one-dimensional heat diffusion equation. The general form of Equation (2.5), for three-dimensional heat flow, is given as;

$$\nabla^2 T + \frac{q_{gen}}{k} = \frac{\rho C_p}{k} \frac{\partial T}{\partial t}, \qquad (2.8)$$

where $\nabla^2 = \left(\frac{\partial^2}{\partial x^2} + \frac{\partial^2}{\partial y^2} + \frac{\partial^2}{\partial z^2}\right)$ is the Laplacian operator.

The governing relationship for heat transfer, in homogeneous isotropic material, is the heat diffusion. The temperature T, within each material section in Fig. 2.6, follows the Equation (2.9)

$$\nabla^2 T = \frac{1}{\alpha} \frac{\partial T}{\partial t}, \qquad (2.9)$$

where T = temperature at location(x,y,z) in the material at time t,

α = thermal diffusivity = $k/(\rho C_p)$,

k = thermal conductivity of the material, *W/(m.K)*,

ρ = specific density, kg/m^3,

C_p= specific heat capacity, *J/(kg.K)*.

The operation ∇^2 when applied to temperature variables in space of the three dimensions gives

$$\nabla^2 = \left(\frac{\partial^2}{\partial x^2} + \frac{\partial^2}{\partial y^2} + \frac{\partial^2}{\partial z^2} \right).$$

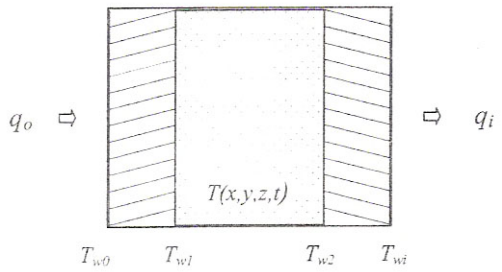

Fig,2.6 Configuration of an opaque wall with multiple layers of homogeneous isotropic materials.

When examining heat transfer across an opaque wall, it is usual to simplify the calculation, by considering a one-dimensional transfer along the depth into the material. In such a case;

$$\frac{\partial^2 T(x,t)}{\partial^2 x^2} = \frac{1}{\alpha} \frac{\partial T(x,t)}{\partial t}. \qquad (2.10)$$

The analysis of heat transfer through the building envelope can be calculated by a number of methods, such as the finite different method, the finite element method and the transfer function method (Petcharat, 2002).

2.4.3 Heat Transfer at the Interior Surface

The net heat flux out of the interior surface of a wall, comprises similar components to those of an exterior surface. An energy balance equation can be written for the heat flux out from the surface, as;

$$q_i = q_{ri} - q_{si} + q_{ci}. \qquad (2.11)$$

Here, the interior surface is exchanging thermal radiation with other surfaces in the room.

CHAPTER 3
METHODOLOGY

3.1 Framework of the Analysis

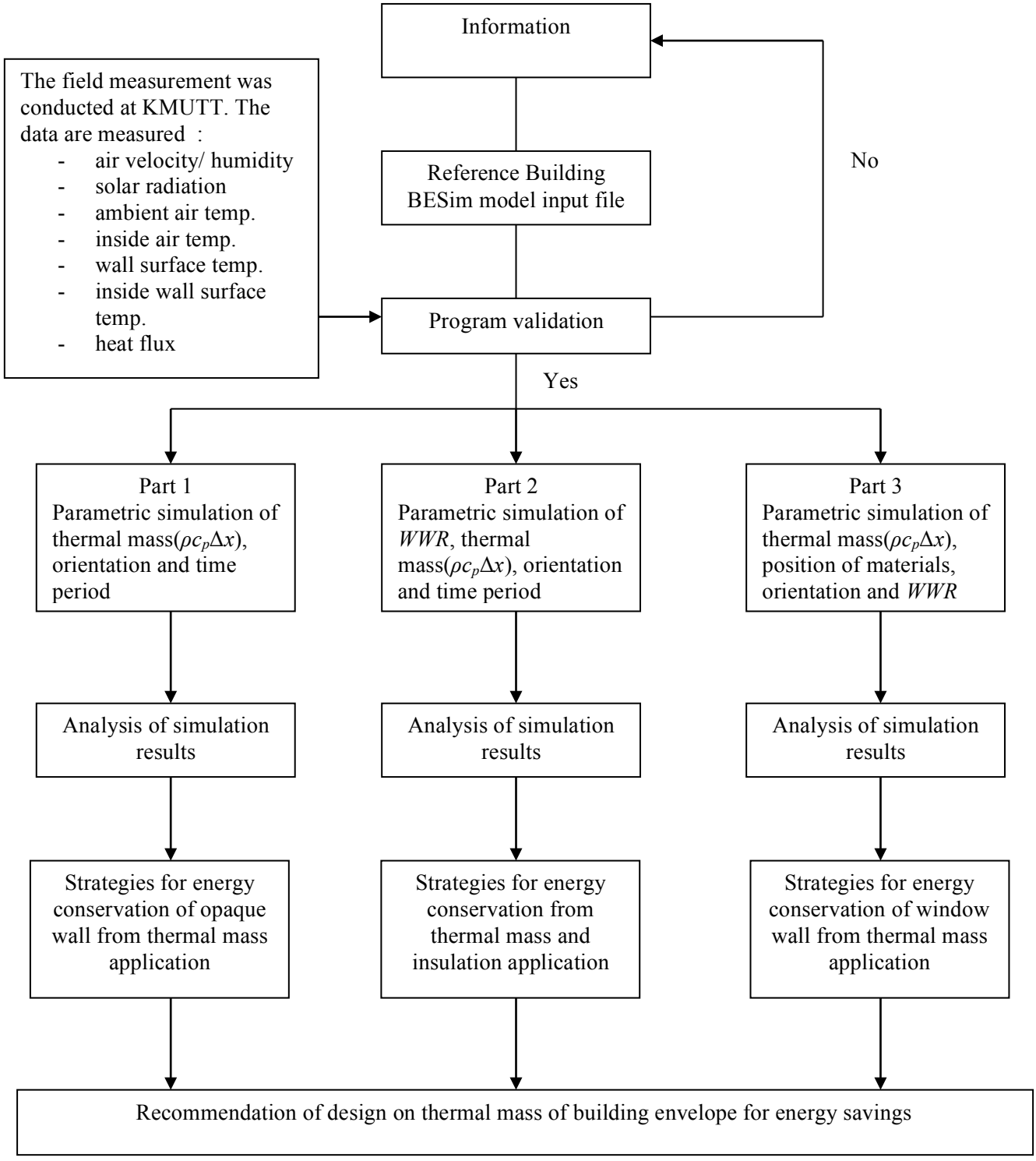

Fig. 3.1 The flow chart of the study

Fig.3.1 is the flow chart of the study. This research thesis investigates the effects of the thermal mass of the building envelope, under different conditions such as orientation, time use of building, and window area to wall area ration *WWR*, by using a simulation method and verifies the simulation program with an actual field experiment. A simulation program, Building Energy Simulation Program : BESim, was used.

According to the objectives of the study, the effect of thermal mass ($\rho c_p \Delta x$) on the building envelope were studied, concentrating on the amount of heat flux passing through the building envelope and the cooling coil load, CCL, of the building. There are 3 sections in this study. Part 1 is an investigation of the appropriate thermal mass on opaque walls, whose parameters are thermal mass quantity, orientation and time period. Part 2 is an investigation of thermal mass effects with different *WWR* on CCL, whose parameters are *WWR*, thermal mass, orientation and time periods. Part 3 is an evaluation of the insulation position of the massive wall, whose parameters are thermal mass, the position of wall materials, orientation and *WWR*. The annual CCL from heat conducting through the wall is a main criterion for evaluating the optimal thermal mass. The result of the study was a recommendation regarding the design of building envelope for energy savings, taking into account thermal mass.

3.2 Methodology

3.2.1 A Building Model for Parametric Study

A building model was created for simulation. A simulation program, Building Energy Simulation Program : BESim, was utilized to calculate the heat flux and the cooling coil load. The simulations were performed continuously over the period of a year, in order to calculate the appropriate thermal mass under various conditions. The accuracy of the simulation model was validated by the experimental results.

The model was square building, and its dimensions is shown in Fig.3.2. There are five rooms, which were called ‘zones’ in simulating, in this building. Zone 1-4 are peripheral zones and zone 5 is a core zone. The peripheral zones were air-conditioned while the core zone was not.

The outer walls, building envelope, were called ‘test walls’ in zone 1-4. These walls faced in different direction; the test wall of zone 1 faced north, the test wall of zone 2 faced

west, the test wall of zone 3 faced south and the test wall of zone 4 faced east. The test walls changed the properties of the wall system, with regard to on parametric simulation. The internal walls of the building were identical, and were constituted of polystyrene foam for insulating heat transfer from other zones, and covered with white-painted gypsum board on both sides. The roof of the building was composed of corrugated cement tiles on the outer side, placed polystyrene foam in the middle and gypsum board at the ceiling. The floor was concrete slabs of 0.15 m. thickness. Only the heat transfer through the test walls had to be taken into account. The composition of each test wall was identical to the others. A building model is shown in Fig.3.2, and the properties of the building materials are shown in Table 3.1.

Table 3.1 The thermo-physical properties of the materials

Type of material	Thickness Δx (cm.)	Conductivity k (W/mK)	Density ρ (kg/m^3)	Specific heat c_p (J/kg.K)	Absorptance	Reflectance
Building envelope						
-test wall	10	0.807	vary	1080	0.5	0.5
Internal wall						
-gypsum	1.2	0.19	879	1088	0.5	0.5
-foam	50	0.035	16	1210	-	-
-gypsum	1.2	0.19	879	1088	0.5	0.5
Roof						
-corrugated tile	0.5	0.198	1860	1000	0.3	0.7
-foam	50	0.035	16	1210	-	-
-gypsum	1.2	0.19	879	1088	0.5	0.5

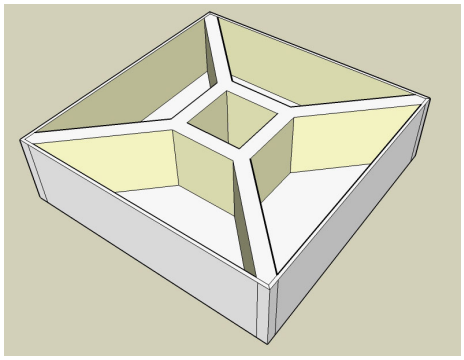

(a)

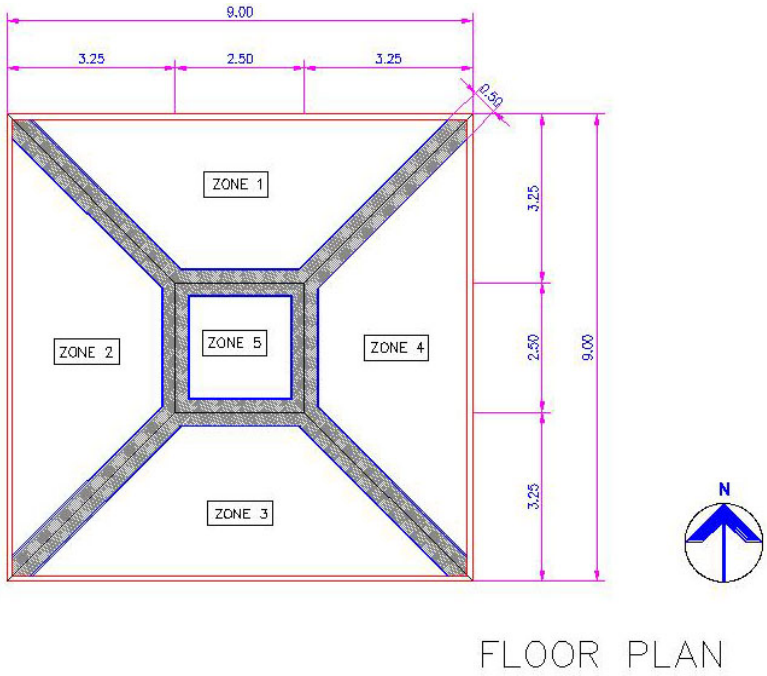

(b)

Fig. 3.2 Configurations of the building model.

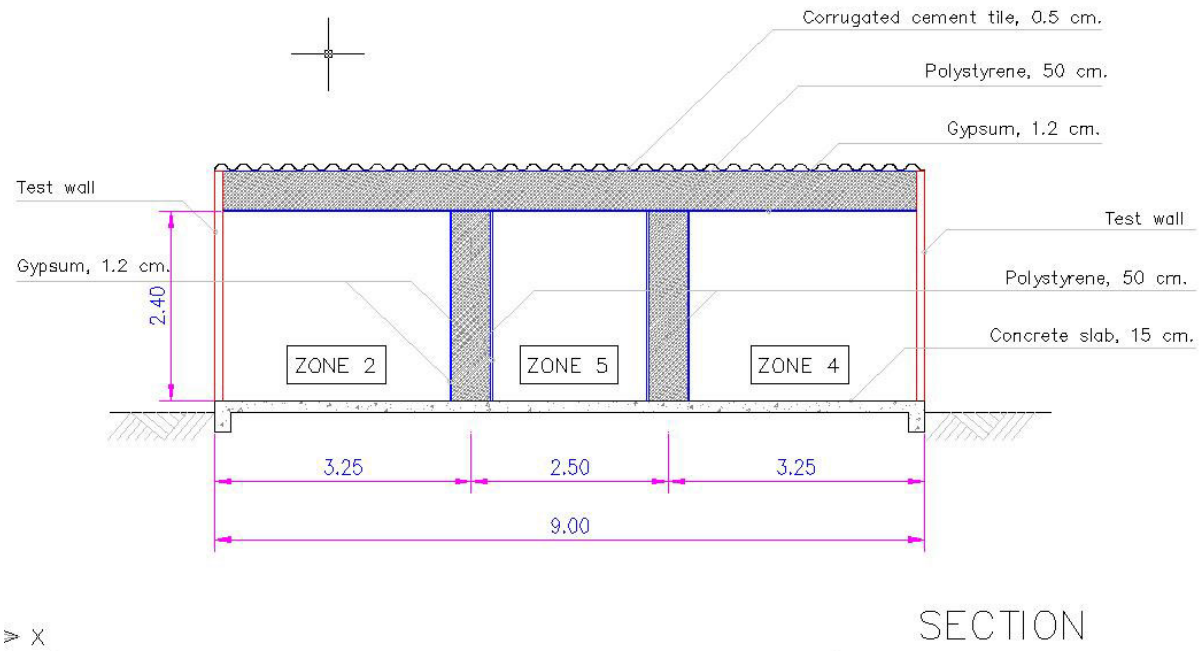

Fig. 3.3 Section of the building model.

3.2.2 The Study Parameters

3.2.2.1 The Optimal Thermal Mass of an Opaque Wall

The models with different the thermal mass values were simulated to find the minimum cooling load in building in cardinal directions. The test walls faced in different directions.

The study considered the various lengths of the operating time period because solar radiation functions with respect to time. The operating time period was varied with the functions and types of buildings. This research studied the effect of thermal mass in four periods of building operating time, as shows in Table 3.2. They consisted of daytime, day and evening, nighttime and 24 hours. The results can apply for the rooms or buildings, in which there was the same operating time. The operating time, was the time during daytime, day and evening, nighttime and 24 hours which an air conditioner was used for controlling the inside temperature .

Table 3.2 Operating time period

Time period	Operating time
Day time (office building)	
- week day	8:00 a.m. – 5:00 p.m.
Day and evening (residential- living & dining room)	
- week day	6:00 p.m. – 10:00 p.m.
- week end	10:00 a.m. – 10:00 p.m.
Night time (residential- bedroom)	
- week day	10:00 p.m. – 6:00 a.m.
- week end	10:00 p.m. – 8:00 a.m.
24 hours (hospital and hotel)	
- week day & week end	24 hours.

The suitable thermal mass was investigated in sixteen situations. They consisted of the situation of the wall faced in cardinal direction, north, east, south and west. For each direction, the simulations were performed in four time periods (4x4=16) as shown in Table 3.3.

Table 3.3 The situation in the study.

Time period	Proper thermal mass			
	North	East	South	East
Day time (office)				
Day and evening (living room)				
Night time (bed room)				
24 hours (hotel & hospital)				

3.2.2.2 The Optimal Thermal Mass under Different *WWR*

The aim of this study was to investigate the effect of the window to wall ration (*WWR*) on the performance of thermal mass, and to find out the suitable thermal mass under different *WWR*. The simulation was run on three *WWR* (0.25, 0.50 and 0.75). The study still considered the operating time and the orientation of the buildings . The annual cooling coil load was a main criterion for evaluating the significant thermal mass. The study was interested in the thermal mass, which influenced significantly the cooling load of the building.

The operating time period in this section was similar two previous parts. The thermal mass was investigated in 48 situations. They consisted of the situation of the wall face in cardinal direction, north, east, south and west. For each direction, the simulations were performed in four time periods, under four *WWR* (4x4x3=48).

The configurations of the experimental model were similar 3.2.2.1, but the test walls were different. Windows were added on the test wall and the dimension of windows were adjusted so that the ratio of the total window area to the total wall area equals to the required value of the *WWR*. The properties of glazing, which was utilized for simulation, shown in Table 3.4.

Table 3.4 Thermo-physical properties of glazing.

Glazing type	Thickness Δx (mm.)	Conductivity k (W/mK)	Density ρ (kg/m^3)	Specific heat c_p (J/kg.K)	Visible transmittance	SHCG
Green float glass	6	1.053	2512	880	0.76	0.54

3.2.2.3 Evaluation of the Insulation Position of the Massive Wall Configurations.

To analyze the influence of the insulation position in the wall system, multilayered walls with orientations that corresponded to the cardinal directions (north, east, south and west) were considered. The simulation was also run under three *WWR* (0.25, 0.50 and 0.75). The investigation was carried out for brick walls (M: d = 14 cm as one layer, or d = 7 cm as two layers), including insulation (I: d = 5 cm as one layer, or d = 2.5 cm as two layers) and coatings on both surfaces (C: d = 1.5 cm). The insulation was assumed to be placed as one layer or two equivalent layers on the outer surface, the inner surface and the mid-center of the brick wall (four wall configurations). These wall formations are defined in Fig.3.4 (Kontoleon et al, 2007). The thickness d and the thermo-physical properties k, ρ and c_p of the said materials, are given in Table 2.5 (DEDE, 2007).

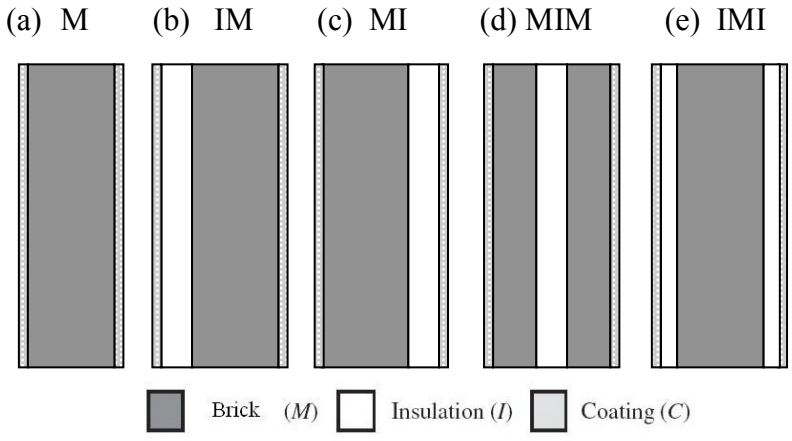

Fig.3.4 Drawing of the wall configurations studied: (a)M, (b)IM, (c) MI, (d) MIM, (e) IMI

Table3.5 Geometrical and thermo-physical properties of the materials that comprising the wall configurations

Type of material	Thickness Δx (cm.)	Conductivity k (W/mK)	Density ρ (kg/m^3)	Specific heat c_p (J/kg.K)
Brick wall (M)	14	0.8	1760	837
Insulation (I)	5	0.035	16	1210
Coating exterior	1.5	0.553	1568	840
Coating interior	1.5	0.553	1568	840

3.2.3 Simulation Program

A simulation program, Building Energy Simulation Program : BESim, was used in this study. It was developed by Vu Duc Hien. The program needed three data files for operating calculation. The data files consisted of a project file, a configuration file and a property file. The project file contained a HVAC system type, a command description for calculation and a parameter print out, and the data of electricity rate. The configuration file contained general data of building such as location, configuration and the zone of the building. The property file was the properties data of the materials which was selected for constructing the building.

There are two calculated programs in BESim, the BuildingFactor01 program which is used for calculating the form factor file and the BuildingEnergy 03 program, which is used for energy calculation. The weather data file of BESim consists of meteorological data and air conditioning system data. The weather data file covers the Thai climate, which was developed by Vu Duc Hien in 2000. The components of BESim are shown in Fig. 3.5

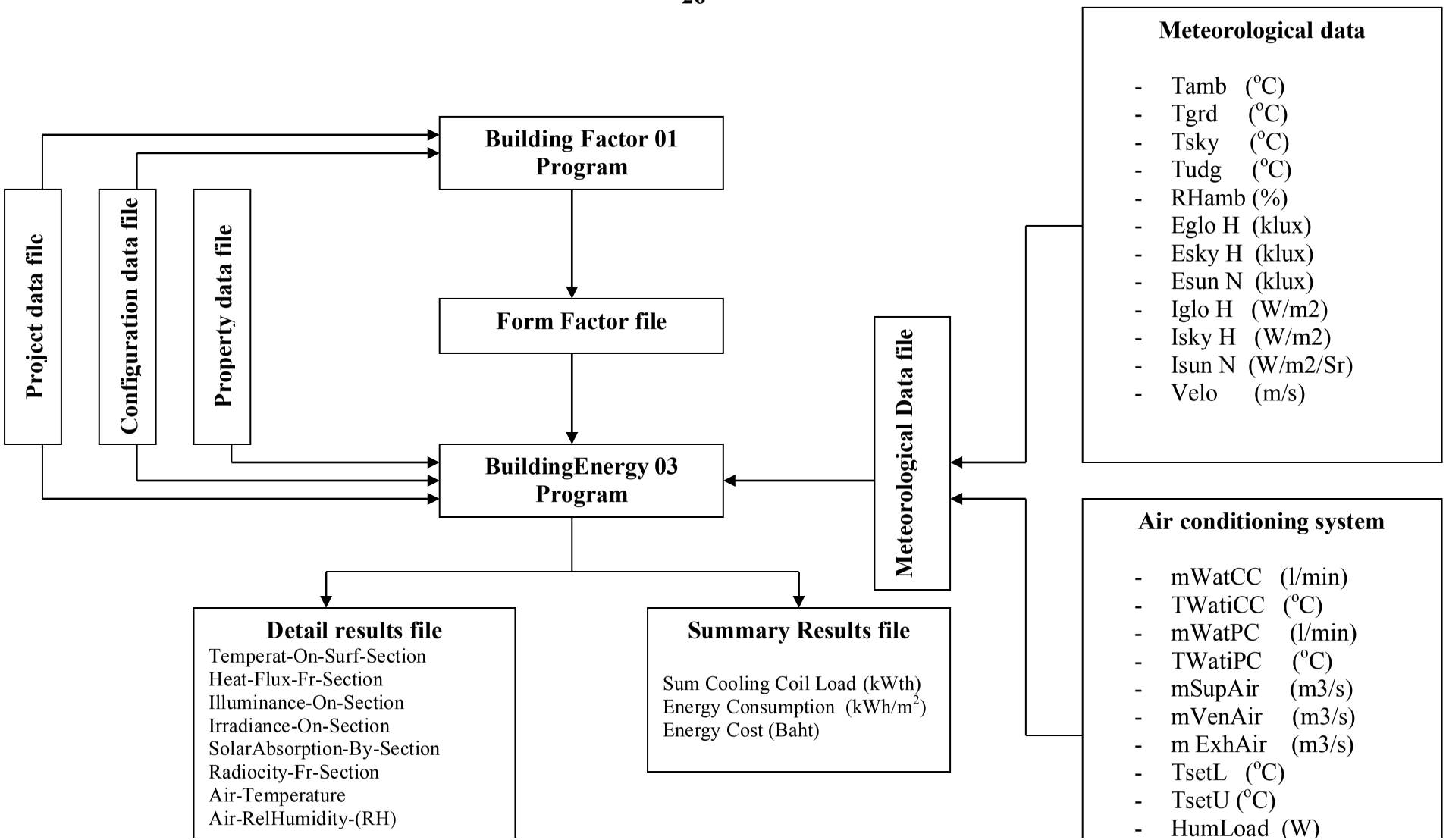
Meteorological data
- Tamb (°C)
- Tgrd (°C)
- Tsky (°C)
- Tudg (°C)
- RHamb (%)
- Eglo H (klux)
- Esky H (klux)
- Esun N (klux)
- Iglo H (W/m2)
- Isky H (W/m2)
- Isun N (W/m2/Sr)
- Velo (m/s)
Building Factor 01 Program
Project data file
Configuration data file
Property data file
Form Factor file
BuildingEnergy 03 Program
Meteorological Data file
Air conditioning system
- mWatCC (l/min)
- TWatiCC (°C)
- mWatPC (l/min)
- TWatiPC (°C)
- mSupAir (m3/s)
- mVenAir (m3/s)
- m ExhAir (m3/s)
- TsetL (°C)
- TsetU (°C)
- HumLoad (W)
Detail results file
Temperat-On-Surf-Section
Heat-Flux-Fr-Section
Illuminance-On-Section
Irradiance-On-Section
SolarAbsorption-By-Section
Radiocity-Fr-Section
Air-Temperature
Air-RelHumidity-(RH)
Summary Results file
Sum Cooling Coil Load (kWth)
Energy Consumption (kWh/m2)
Energy Cost (Baht)

3.2.4 Designs of Experiment and Validation

The energy fluxes through the wall were simulated and compared with the data from the field measurement, in order to verify the program's validity and reliability . The field experiment was set up in the building which is located on Bangkunthien campus, King Mongkut's University of Technology Thonburi, Bangkok.

Fig.3.6 The experimental building

3.2.4.1 Experimental Descriptions

The building was located at latitude 13.73^{o}N and longitude 100.5^{o}E. It was three storeys high and its dimension were 6.00 m. x 6.00 m. x 15.00 m. The roof of the building was of concrete slab. The front of building faced south. Fig.3.7 shows a schematic diagram of the testing room. The external surface and internal surface of the building envelope were attached with a temperature sensor, J-type thermocouple. The measuring temperature obtained on each surface was assumed to represent an average temperature of the surface. Inside the room, a J-type thermocouple was installed in the middle of the room. Another J-type thermocouple was buried 5 cm. under the ground surface, for measuring ground surface temperature, and it was placed about 3 meters away from the building. A weather station was set up on the roof deck. The experimental building consisted of :

(a). A building envelope facing west, on the 2nd floor was used as the test wall. It was a brick wall, a conventional building wall in Thailand, with 10 cm. thickness. Both the inner and outer surfaces of the test wall were plastered with cement mortar and painted white.

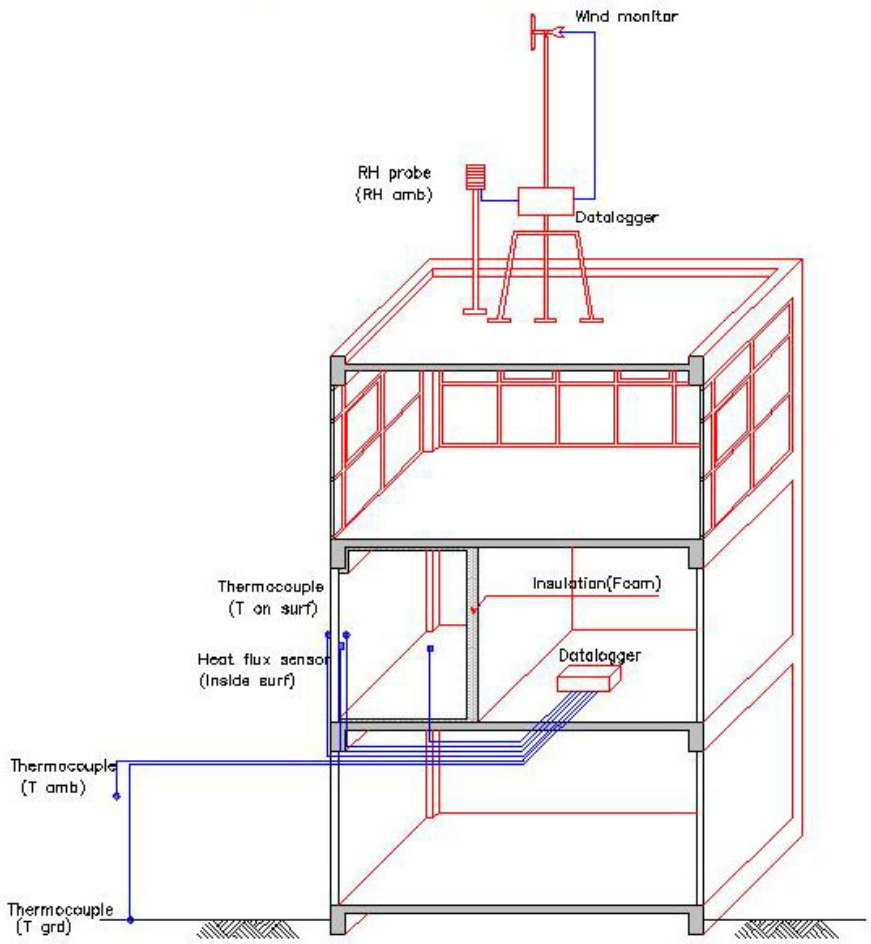

Fig.3.7 A schematic diagram of the test room

(b). A air-conditioner with 18300 BTU/hour, which served to keep the temperature at 26^{o}C.

Fig.2.8 Air-conditioner in the test room

(c). A weather station was set up on the roof deck. It consisted of a “RM Young 05103”, for measuring the speeds and direction of winds, and a “Vaisala CS500-U” for measuring the ambient temperature and the relative humidity. A Campbell data logger “CR10X” was used to monitor and record weather data, by programming it to sample data every 10 seconds, and averaging the sampling data for an average hourly value in each hour.

Fig.2.9 Weather station on the roof deck

(d). A Kipp & Zonen “CM11” was mounted on the roof deck for measuring the solar radiation.

Fig.2.10 pyranometer

(e). This research used a thermocouple type J as a temperature sensor. Temperature measurements were conducted at ground surface, underground, on the external surface wall, on the internal surface wall and also the internal air temperature.

External and internal surface walls were attached with J-type thermocouple. The surface wall had been painted with conductive silicone before the thermocouple was

installed and covered with aluminium tape. The aluminium tape on the external surface wall was painted white for protecting thermal transfer from the aluminium tape to the thermocouple, when the aluminium tape exposed to the sun. For internal air temperature measurement, the thermocouple was covered with an aluminium foil cone at the end of thermocouple to protect the blowing air from the air conditioner.

(a) Thermocouple installation on the test wall.

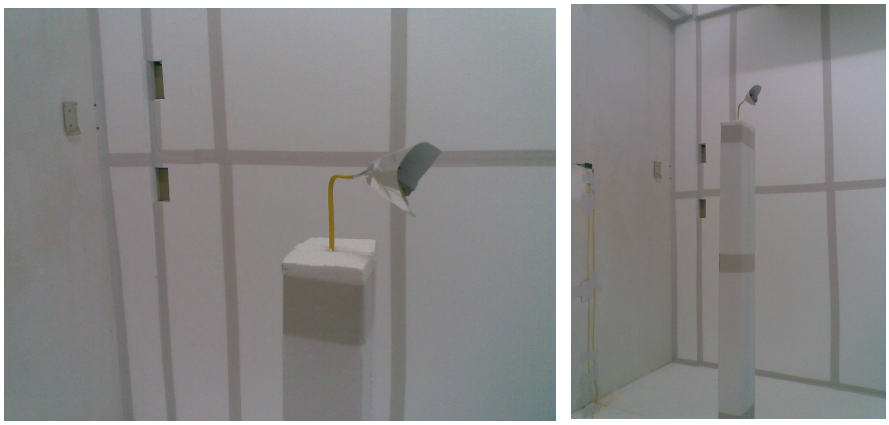

(b) Thermocouple in the middle of the room

(c) Thermocouple at ground surface and on the outside building

Fig.3.11 Thermo couple installation

(f) Heat flux sensors were used for heat flux measurement on the inner wall surface. The data of temperature and heat flux were recorded by a data logger (Yokogawa, DC-100)

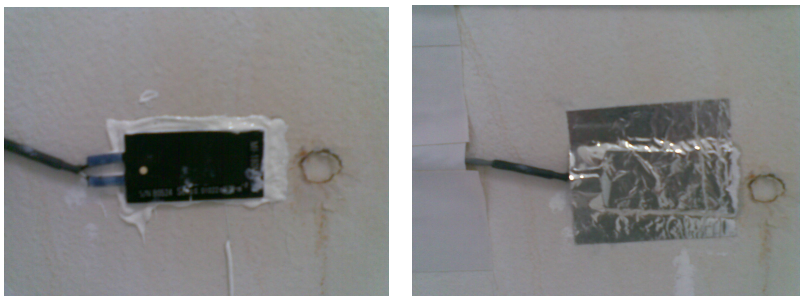

(a) Heat flux on the internal surface

(b) Data collector (Yokogawa, DC-100)

Fig.2.12 Heat flux sensor and data collector

3.2.4.2 The Test Room Configuration

A test room on the second floor was constructed for the experiment. The test room's dimensions were 2.50 m. x 3.00 m. x 3.00 m. The walls of this room were opaque wall. The west wall was used as test wall and it was a brick wall of 10 cm. thickness. The north wall was two layers of cement board, 0.3 cm. thickness at each layer, with a middle air gap of 8 cm. thickness and insulated with 15 cm. polystyrene foam. The internal walls are polystyrene foam, 15 cm. thickness. The concrete floor and ceiling were insulated with 5 cm. polystyrene foam. The test room is shown in Fig.3.13 and Fig. 3.14.

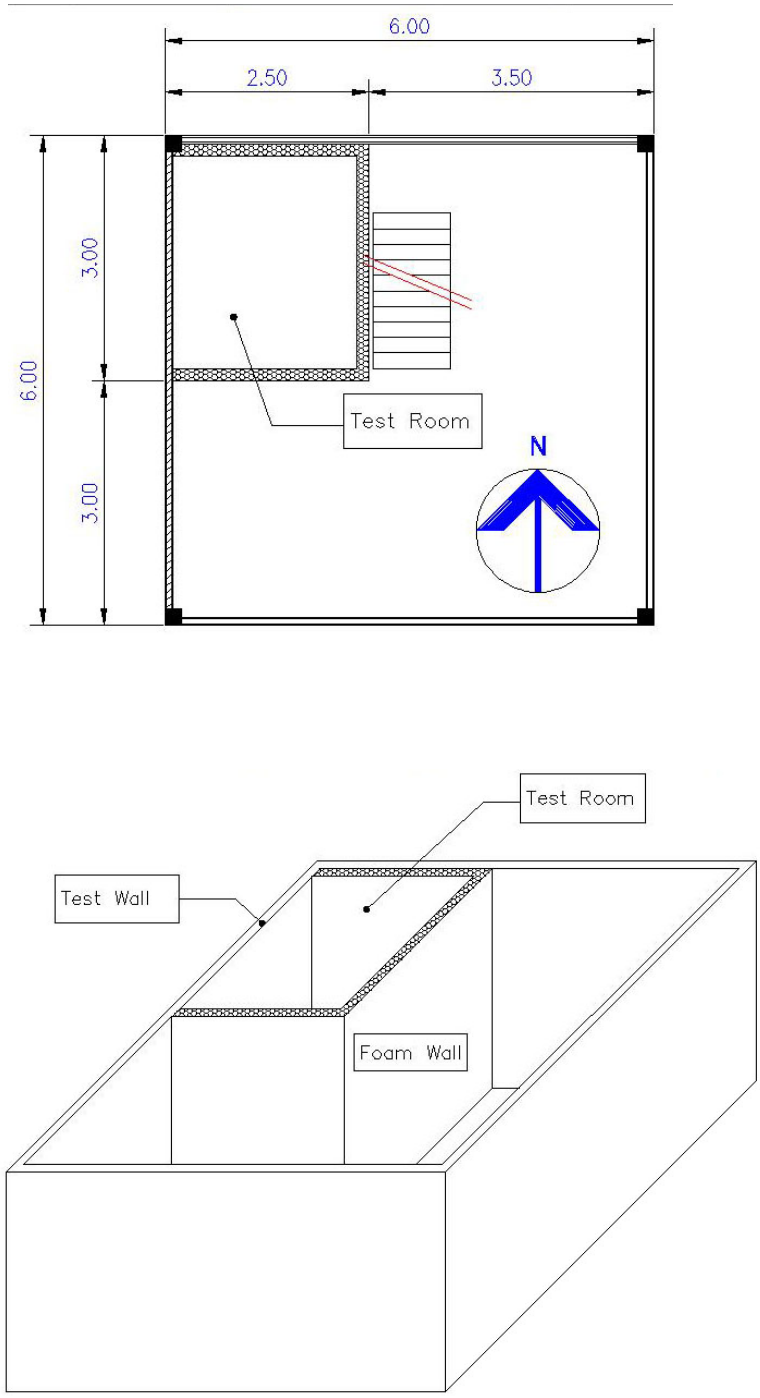

Fig.3.13 Plan and isometric drawing of the test room

Fig.3.14 The test room was constructed on the 2nd floor of the experimental building.

3.2.4.3 Validation

The aim of the field experiment is to validate the accuracy of the simulation program. A similar building was created to be the simulation model. Data from the field experiment was recorded and used as input parameters for simulating the model. The data of the experiment had been recorded continuously for a week.

The parameters of the test wall surface were considered. The heat flux at the inner surface was used for verifying the accuracy of the simulation. Measured heat fluxes and calculated heat fluxes were plotted with respect to time in hours on the same axis. The validation is assessed by method of statistical analysis, in which the root mean square error (RMSE) and the mean bias error (MBE) were applied for validation.

The Root Mean Square Error (RMSE) was calculated from the sum of the square of the difference between the simulated heat fluxes and the measured temperatures. Positive values of the RMSE were obtained and the RMSE was used to quantitatively assess the accuracy of prediction results, compared with experimental results, as shown in Equation (3.1).

$$RMSE = \left[\frac{\sum_{t=1}^{N} (H_{cal} - H_{meas})^2}{N-1} \right]^{1/2} \tag{3.1}$$

where H_{cal} is the calculated heat flux, W/m^2,

H_{meas} is the measured heat flux, W/m^2,

N is the total number of observation.

The Mean Bias Error (MBE) was used to examine the presence and the direction of bias in forecasts or systematic errors of predictions. MBE provided either positive or negative values. A positive MBE indicated that model calculations tend to over-predict and vice versa. The MBE is in the equation below,

$$MBE = \left[\frac{\sum_{t=1}^{N} (H_{cal} - H_{meas})}{N-1} \right] \tag{3.2}$$

CHAPTER 4
RESULTS AND DISCUSSION

This chapter represents the results and discussion of the study. The accuracy of the simulation program verified for the surface heat flux of the test wall, and the performance of the thermal mass on the cooling coil load, CCL, were studied by simulation techniques under various parameters, as mentioned in the previous chapter.

4.1 Verification of the Simulation Program and Its Accuracy

The program was assessed for its capability to predict accurate surface heat flux. The heat fluxes on the inner surface of the test wall are taken into account for evaluating the program's accuracy. Hourly heat fluxes on the test wall surface in the field experiments were measured over entire days at Bangkuntien Campus, King Mongkut's University of Technology Thonburi (KMUTT), Bangkok, Thailand at latitude 13.73^{o}N and longitude 100.5^{o}E and compared with the simulated hourly heat fluxes.

Four days are selected to present the results in Fig.4.1. The operating times of the air conditioner in the test room are shown in Table 4.1. The data logger was set to receive the input signal range between 0-20 mV. Actually, it should have been set to receive a negative signal as well. Thus, the evaluation calculated only the hourly heat fluxes during the air conditioning period. Fig.4.1 illustrates the measured and the simulated heat fluxes.

Table 4.1 Operating times of the air conditioner in the test room

Date	Operation time
6 May 2009	12.00 – 18.00
7 May 2009	11.00 – 17.00
9 May 2009	10.00 – 24.00
10 May 2009	00.00 – 15.00

For the program validation, the first simulation give the results in the overestimation of the heat flux prediction on the inner surface (back surface) of the test wall, as shown in Fig. 4.1(b). The overestimation is due to the incorrect value, which is not consistent with the actual wall data, of the test wall properties on the input data. When changing some properties of the test wall on the input data, the simulation give results which tally closely

with the measurement results, as shown in Fig 4.1(c). The test wall property data, which are changed in the simulation, are shown in Table 4.2.

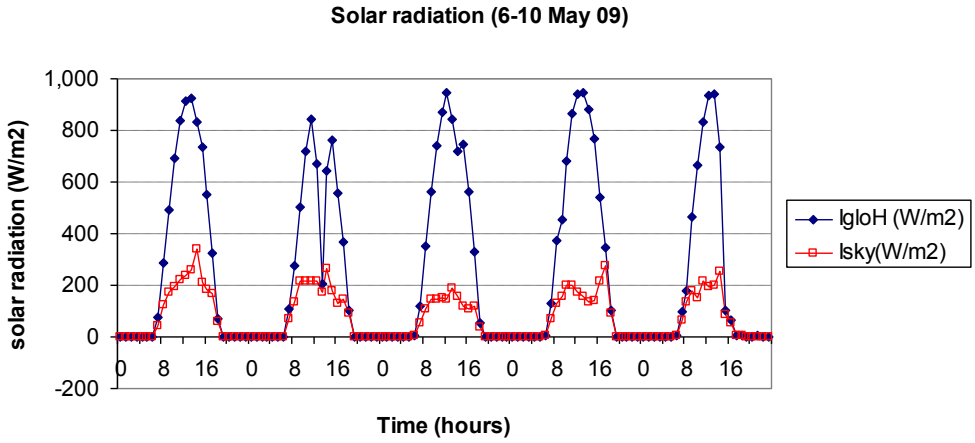

(a) Global and diffuse solar radiation on the horizontal surface

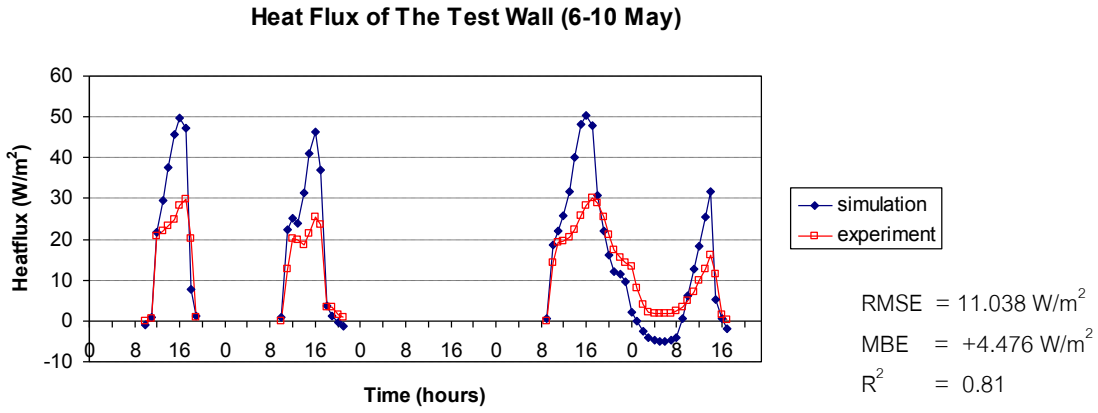

(b) Heat flux on the inner surface of the test wall (before changing the wall properties)

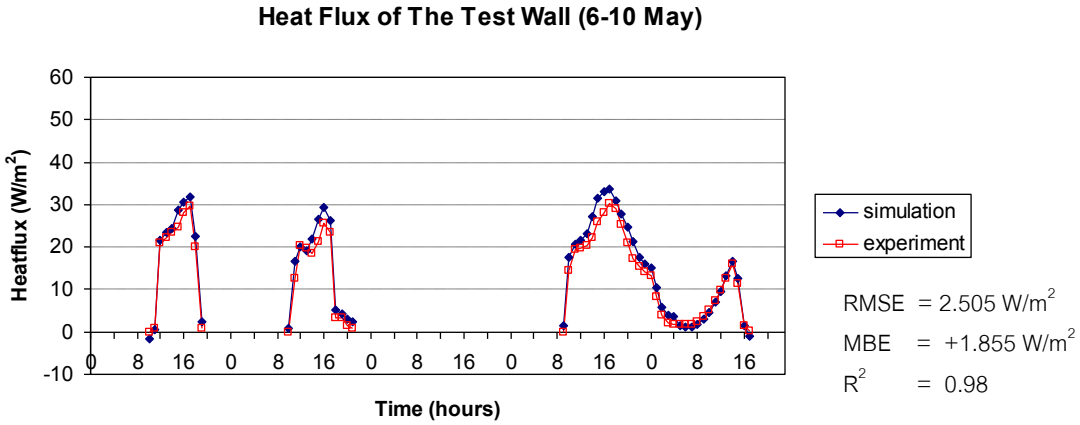

(c) Heat flux on the inner surface of the test wall (after change the wall properties)

Fig 4.1 Hourly heat flux profiles of measured and simulated heat fluxes

In Fig.4.1(c), the values of the simulated heat flux are slightly higher than the heat flux values of the experiment. The validation of the accuracy of the program indicates that the prediction preformed relatively well and agreed with the measurement results on the inner surface, with the average of RMSE is 2.505 W/m^2 and +1.855 W/m^2 of MBE. Fig. 4.1 represents not only the accuracy of the program, but also the behavior of the heat flux response of the wall with the input solar radiation. The square of the correlation coefficient R^2 of the predicted heat fluxes on the inner surface of the test wall is 0.98. It can be explained that a result greater than 98% of the total variation in prediction temperatures, would have a linear relationship with the measurement results.

The profile heat fluxes are dynamic with changes in the solar irradiance showing the same trends as the measurement data. On 9 May, the maximum solar radiation was around 1.00 pm while the peak of heat flux of the inner surface occurred at around 5 pm. The maximum heat flux of the inner surface of the west wall shifted to the late afternoon, which was a four-hour time lag.

Table 4.2 The input data of wall properties on the validation of the simulation program

Wall properties	Input Data	
	Before change	After change
Thickness (m)	0.1	0.13
Conductivity (W/mK)	0.807	0.807
Density (kg/m3)	1,760	1,760
Specific heat (J/kgK)	837	1,200
Front absorptance	0.5	0.3
Front reflectance	0.5	0.7
Back absorptance	0.5	0.5
Back reflectance	0.5	0.5

4.2 Results of finding the optimal thermal mass of the opaque wall

In this section, the result of the parameters, thermal mass and operating time periods, are discussed. The analyses are conducted for wall configurations, mentioned in the previous chapter, and for the cardinal directions.

4.2.1 Operation time period in the daytime

The heat flux through the wall and the cooling coil load, CCL, in zones 1-4 are simulated as a function of the amount of thermal mass of the test wall. The CCL of the room are influenced by heat gain from the test wall. The operation time period of the air conditioner in the building is assumed from 8:00 a.m. until 5:00 p.m., on weekdays.

Fig.4.2 shows the heat flux on the inner surface wall in the northerly direction, on 28 May – 29 May. The value of the heat flux decreases when the value of thermal mass increases. The heat flux value of the light mass shows more fluctuation than the heavy mass. The solar heat is stored in the thermal mass during the daytime, so that the heat flux peak of the heavy mass is lower than that of the light mass. During the time period when the air conditioning is not being operated, the value of heat flux entering into the room decreases and there are negative values at night in some thermal masses, particularly the light mass. For the very heavy thermal mass, the emission of the stored heat at night is delayed until the next morning and causes the high CCL value at the beginning of the next day.

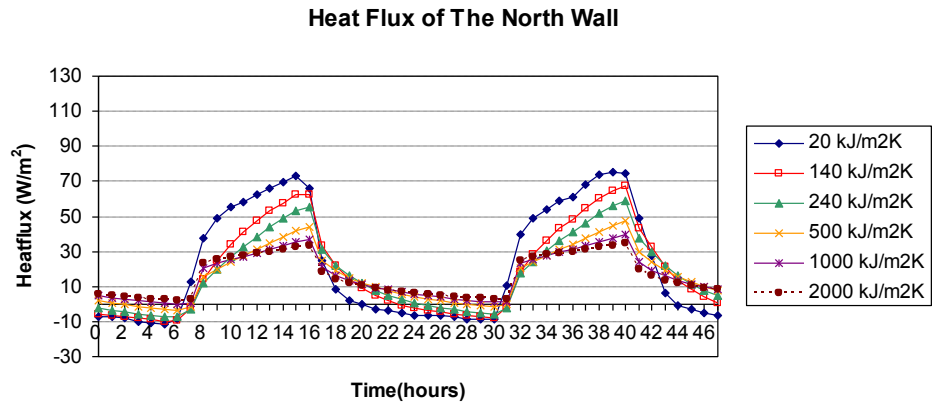

(a)

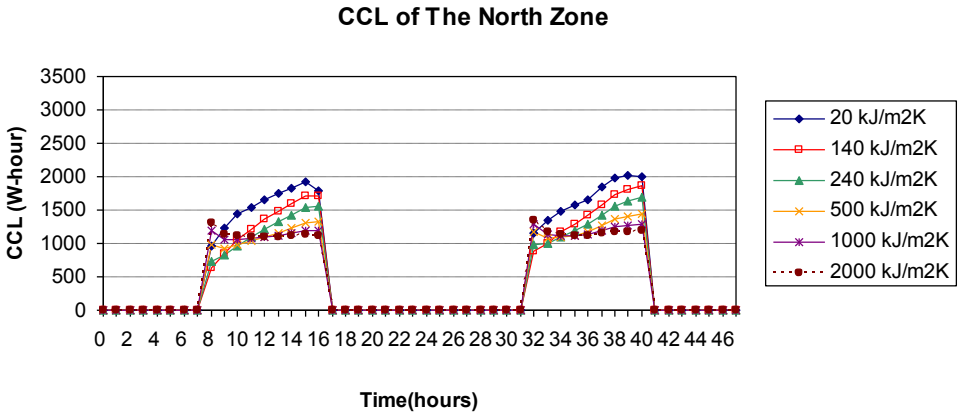

(b)

Fig. 4.2 Heat fluxes flow through the north wall and the CCL of the north zone on 28 May – 29 May

In Fig. 4.2, the heat fluxes are related to the cooling coil load, CCL, of the test room. The values of CCL increase when the value of the heat flux increases. While the value of heat flux decreases, the value of the CCL also decreases. The CCL value of the light mass shows more fluctuation than the heavy mass. These phenomena also occur in the other directions, as shown in Fig 4.3-4.5. The values of maximum heat flux on the west wall and the east wall are higher than the north and the south wall.

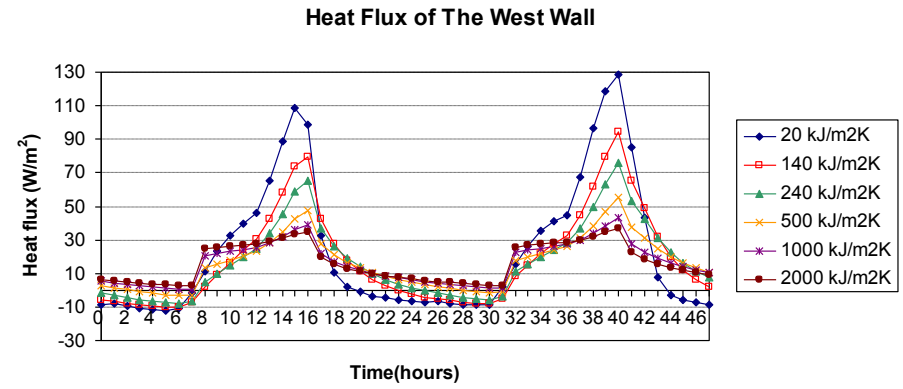

(a)

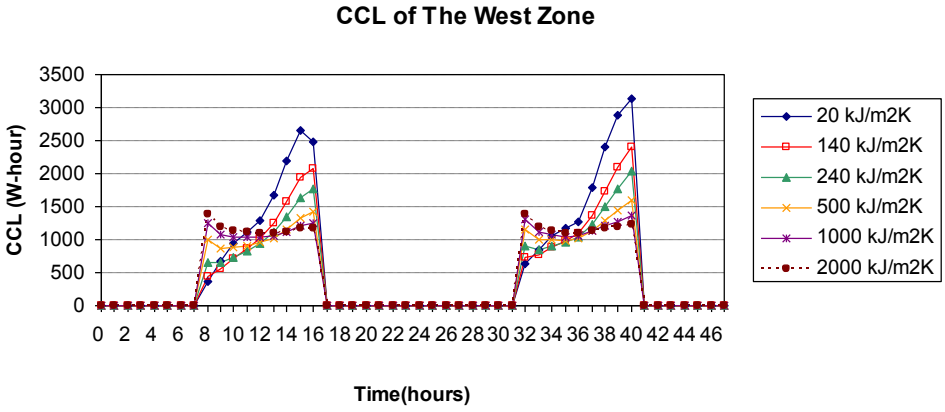

(b)

Fig. 4.3 Heat fluxes flow through the west wall and CCL of the west zone on 28 May – 29 May

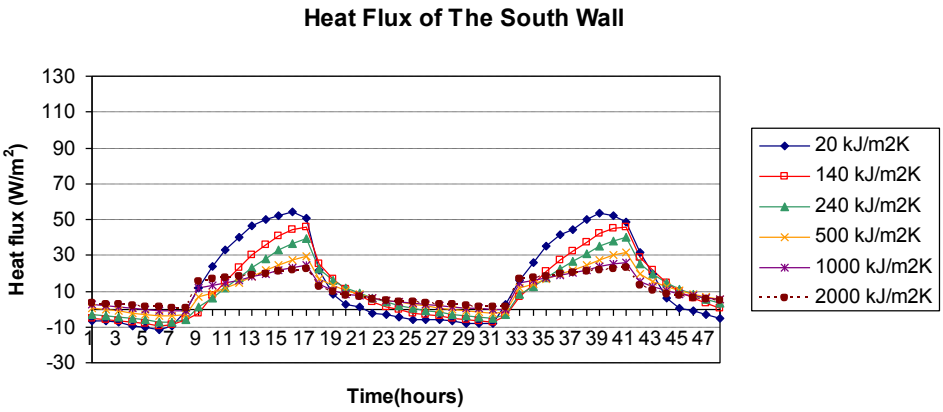

(a)

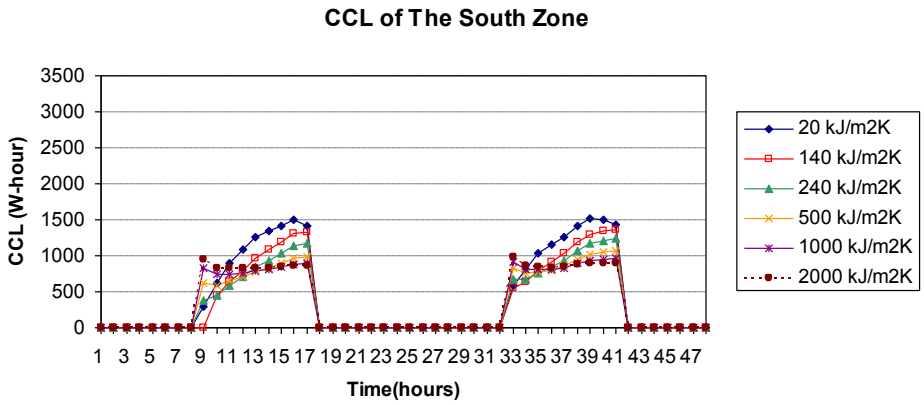

(b)

Fig. 4.4 Heat fluxes flow through the south wall, and the CCL of the south zone on 28 May – 29 May

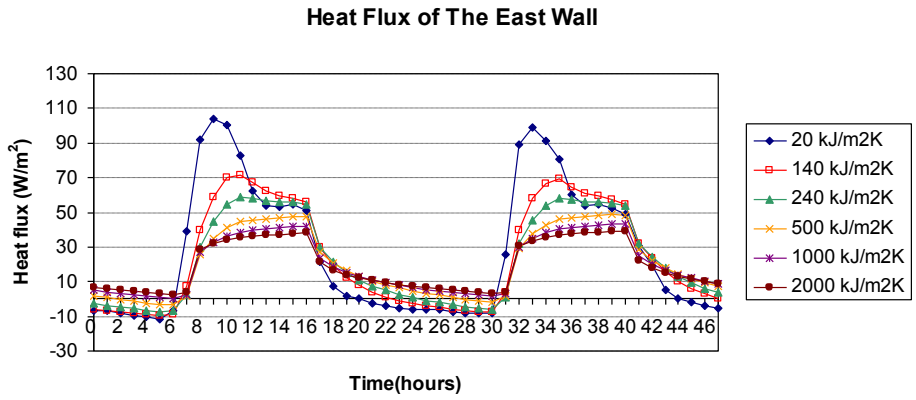

(a)

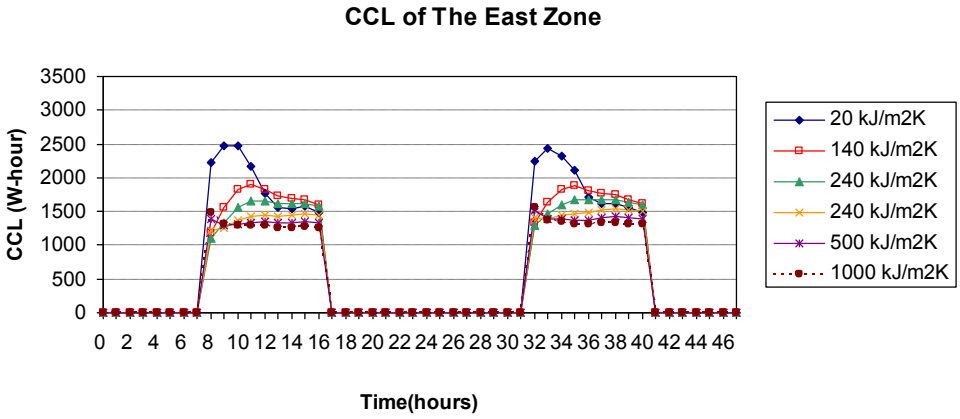

(b)

Fig. 4.5 Heat fluxes flow through the east wall and CCL of the east zone on 28 May – 29 May

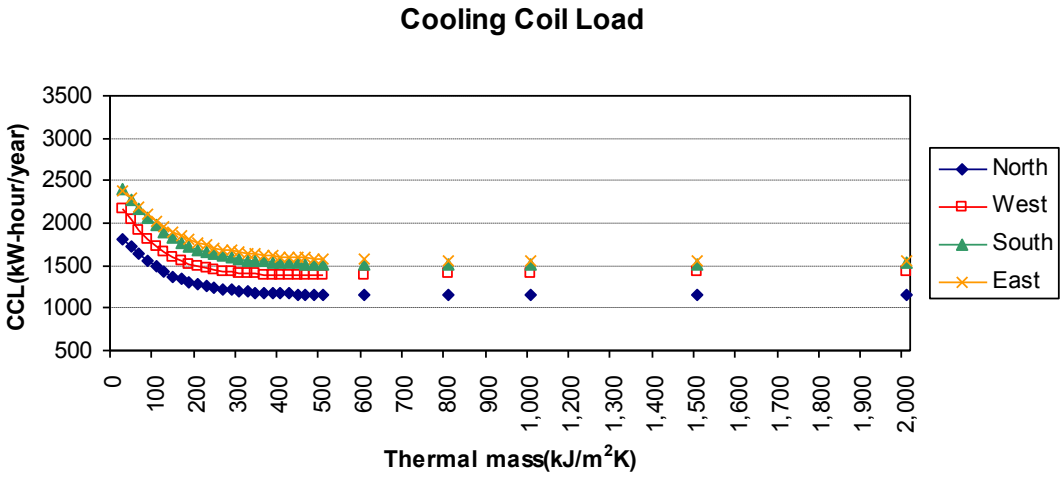

Fig.4.6 The annual CCL in each direction under turning the air conditioner on at day time

Fig.4.6 shows clearly that the east wall has the most annual CCL. The south and the west walls have less annual CCL, respectively. The north wall has the lowest annual CCL. It indicates that the north facing wall minimizes heat gain through the wall, and heat gain is maximum on the east facing wall. The annual CCL in each zone decreases when increase the thermal mass of the test wall increases. The CCL is clearly reduced when the thermal mass increases from 20 kJ/m^{2}K to 300 kJ/m^{2}K. For 300 kJ/m^{2}K -600 kJ/m^{2}K, the CCL in every zone shows a small reduction. For 600 kJ/m^{2}K - 1000 kJ/m^{2}K, the CCL are lowest. For larger values of thermal mass, the CCL increases again.

Fig.4.7 shows the annual CCL of the building. The annual CCL decreases very clearly for thermal mass 20 kJ/m^{2}K – 300 kJ/m^{2}K and then the annual CCL show a small reduction when the value of thermal mass increases. At 600 kJ/m^{2}K, the annual CCL is the lowest at 5,621.52 kWh/year. The annual CCL increases again for the larger thermal mass. For 300 kJ/m^{2}K and 600 kJ/m^{2}K thermal mass, the CCL is reduced to 33.17% and 35.75%, respectively, when compared to the CCL of the 20 kJ/m^{2}K thermal mass. The suitable thermal mass for this case is about 300 kJ/m^{2}K.

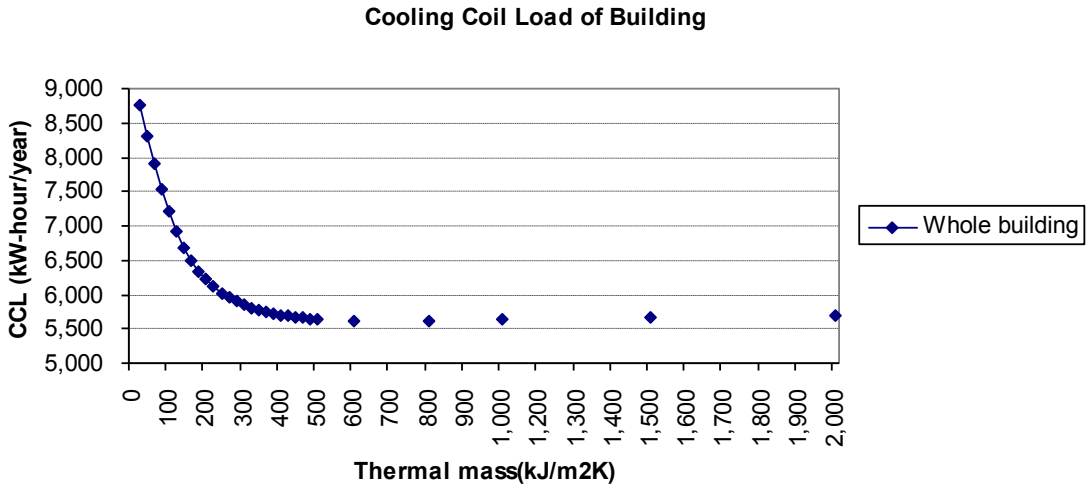

Fig.4.7 The annual CCL of buildings when the air conditioning is switched on during the day.

4.2.2 Operating time period in the evening and during the day

The operating time period of the air conditioner in building for this case is assumed from 6:00 p.m. until 10:00 p.m. on weekdays, and from 10 a.m. until 10:00 p.m. at weekend. The results of the heat flux through the wall in each direction, simulated on 28 - 29 May, are shown in Fig. 4.8 – Fig. 4.11.

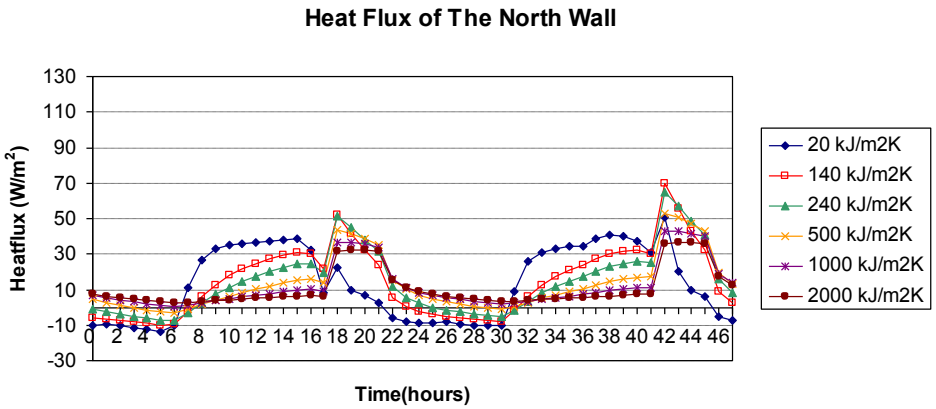

(a)

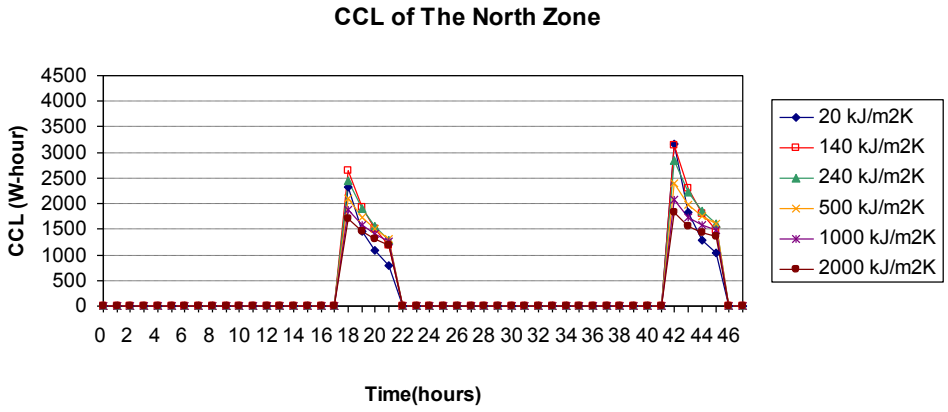

(b)

Fig. 4.8 Heat fluxes flow through the north wall and the CCL of the north zone on 28 May – 29 May.

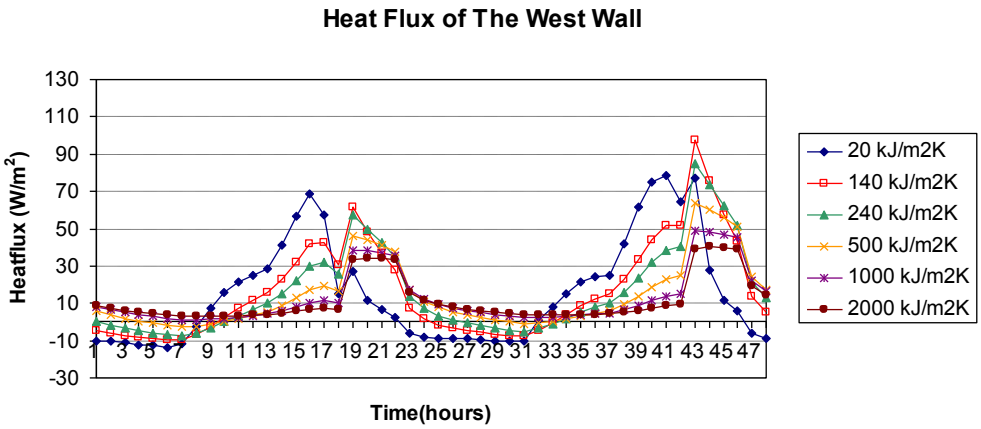

(a)

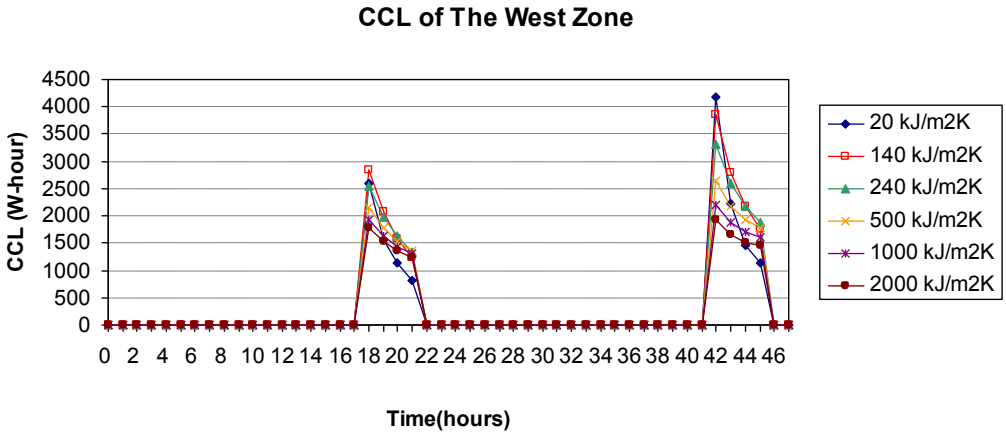

(b)

Fig. 4.9 Heat fluxes flow through the west wall and the CCL of the west zone on 28 May – 29 May

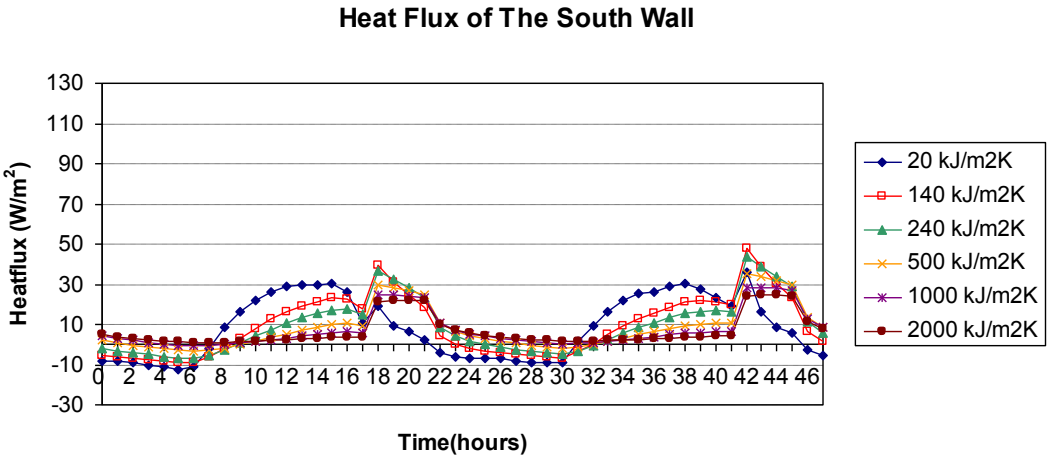

(a)

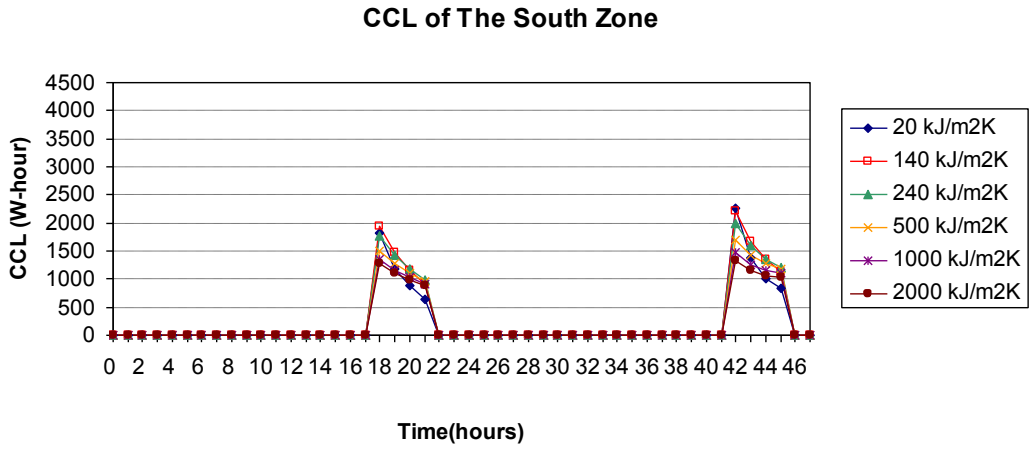

(b)

Fig. 4.10 Heat fluxes flow through the south wall and the CCL of the south zone on 28 May – 29 May

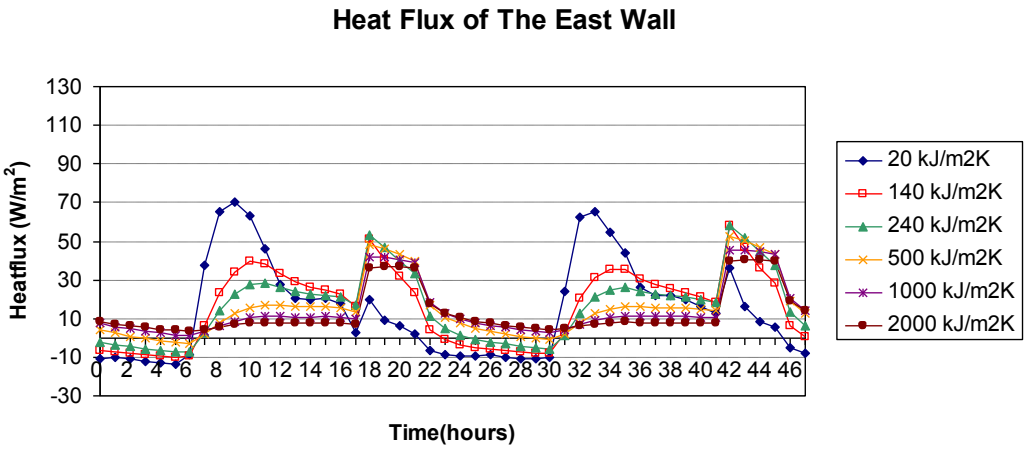

(a)

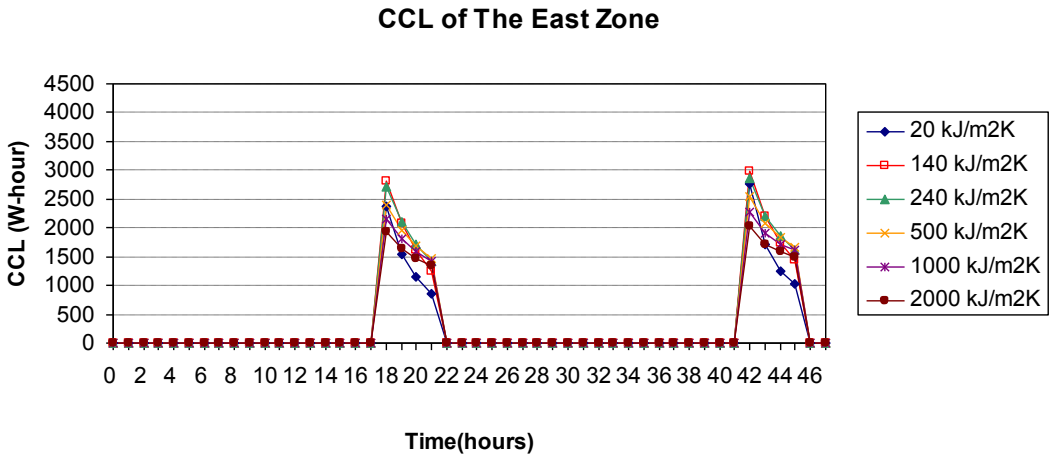

(b)

Fig. 4.11 Heat fluxes through the east wall and the CCL of the east zone on 28 May – 29 May.

Fig.4.8 - Fig.4.11 show heat flux flow through the inner wall surface under when the air conditioner is switched on in the evening. When switching the air conditioner on, the heat flux is high at the beginning and then decreases later on. The heat flux values of the 140 kJ/m^{2}K and 240 kJ/m^{2}K thermal mass are high at the beginning, and then they decrease rapidly later on. For the very heavy thermal mass, the heat flux values are lower at the beginning but they exhibit a small reduction. As for the small amount of thermal mass (20 kJ/m^{2}K), its heat flux is lowest because it has a small heat storage capacity so the heat is released more rapidly than the others .

Fig.4.12 illustrates the annual CCL with the air conditioner is switched on during the daytime and evening. For 20 kJ/m^{2}K- 120 kJ/m^{2}K thermal mass, the annual CCL increases when the value of the thermal mass increases. The annual CCL of the north zone are obviously lower than the CCL of other zones. For the north zone, the highest CCL is 1,663.72 kWh/year when the thermal mass is 120 kJ/m^{2}K. For the west zone, the highest CCL is 2,143.89 kW/year when the thermal mass is 100 kJ/m^{2}K. When thermal mass is 140 kJ/m^{2}K, the highest CCL is 2,153.62 kWh/year and 2,064.52 kWh/year for the south zone and the east zone, respectively. For the larger thermal mass, the CCL decreases when the value of the thermal mass increases.

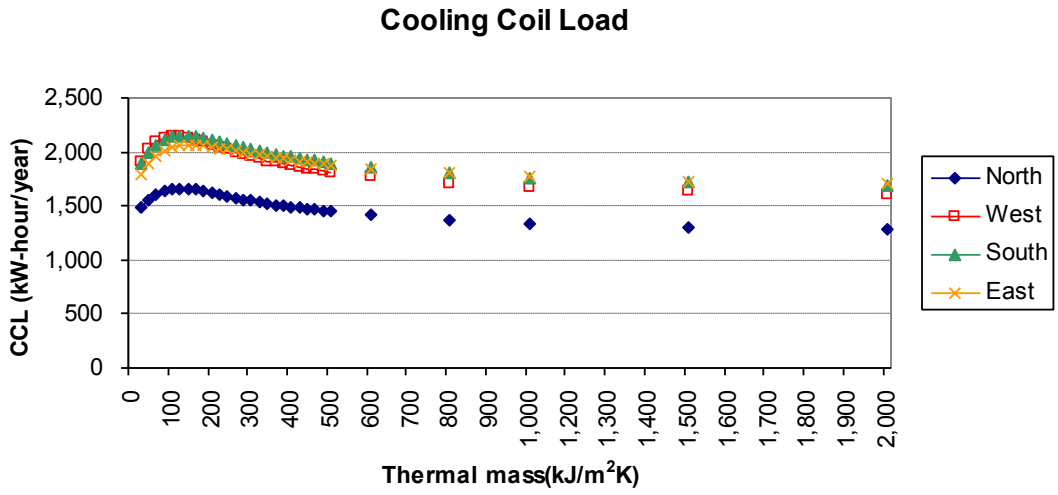

Fig.4.12 The annual CCL in each direction when the air conditioning is on at the daytime and evening

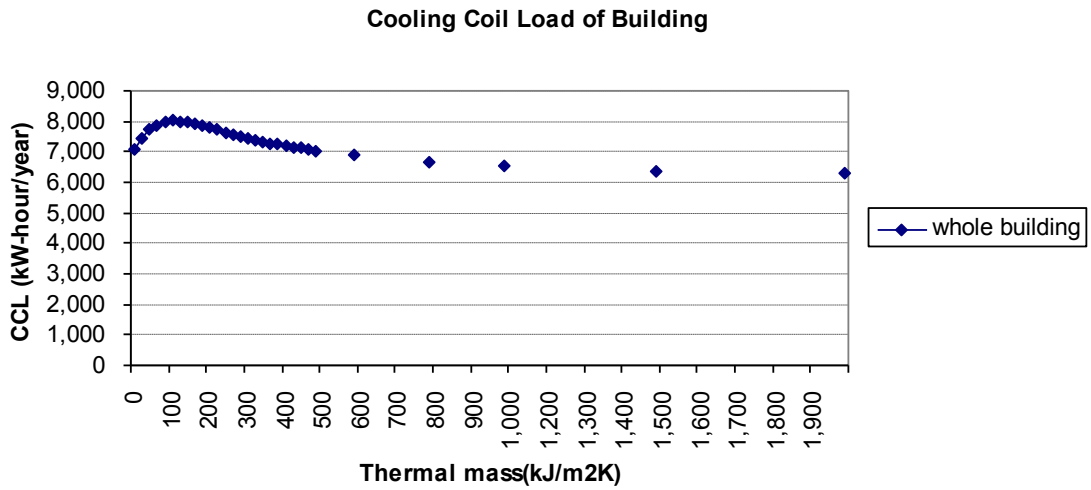

Fig.4.13 The annual CCL of building when the air conditioning was switched on at the daytime and evening

Fig.4.13 shows the annual CCL of the whole building when the air conditioning is on during the daytime and the evening. The annual CCL increases when the value of thermal mass increases from 20 kJ/m^{2}K to 120 kJ/m^{2}K. When the thermal mass is 120 kJ/m^{2}K, the annual CCL is highest at 8,018.74 kWh/year. For the larger thermal mass, the annual CCL decreases when the amount of thermal mass increases. For thermal mass of 100 kJ/m^{2}K, the CCL increased to 12.57%, when compared to the CCL of 20 kJ/m^{2}K thermal mass.

4.2.3 Operating time periods at night

The operation time periods of air conditioner in the building in this case is assumed from 10:00 p.m. until 6:00 a.m. on weekdays, and from 10 p.m. until 8:00 a.m. on the week end.

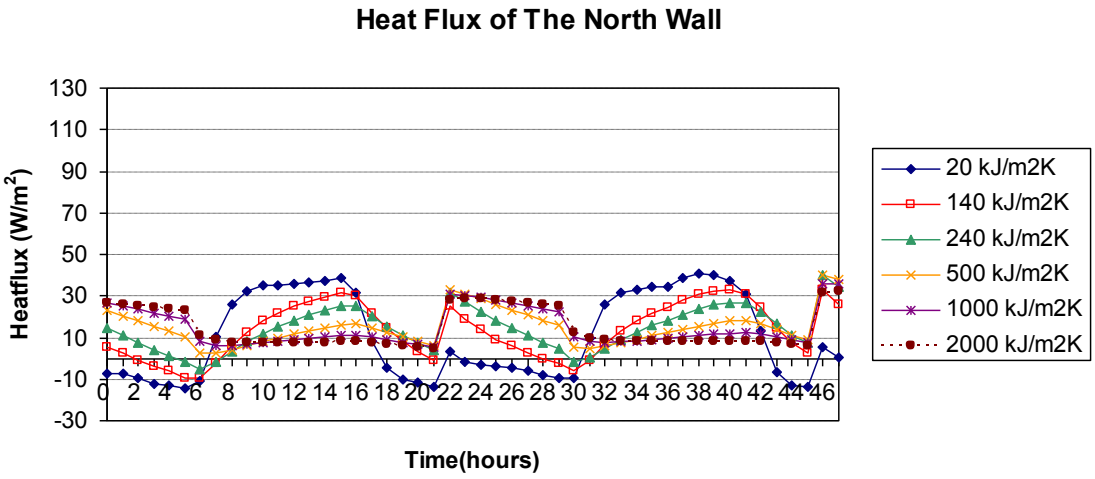

(a)

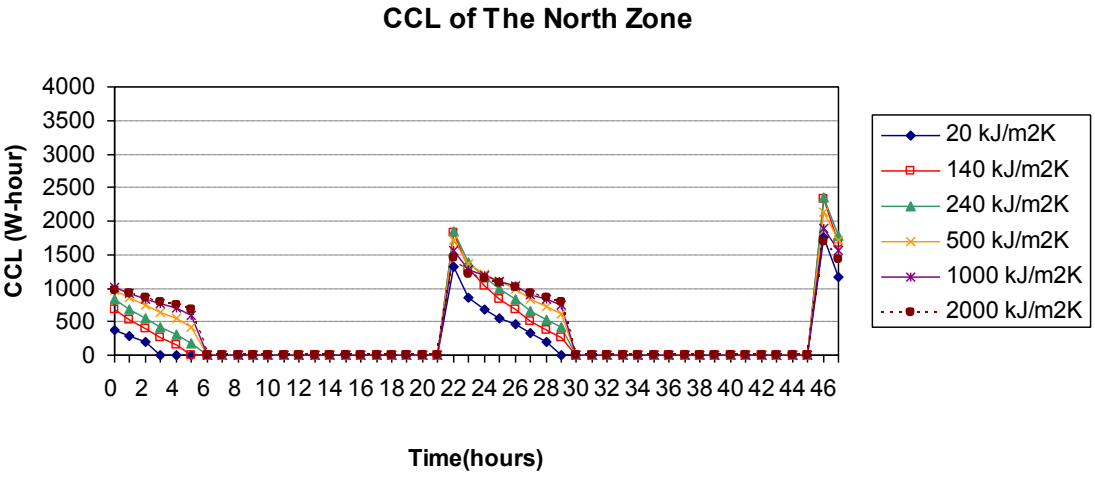

(b)

Fig. 4.14 Heat fluxes flow through the north wall and the CCL of the north zone on 28 May – 29 May

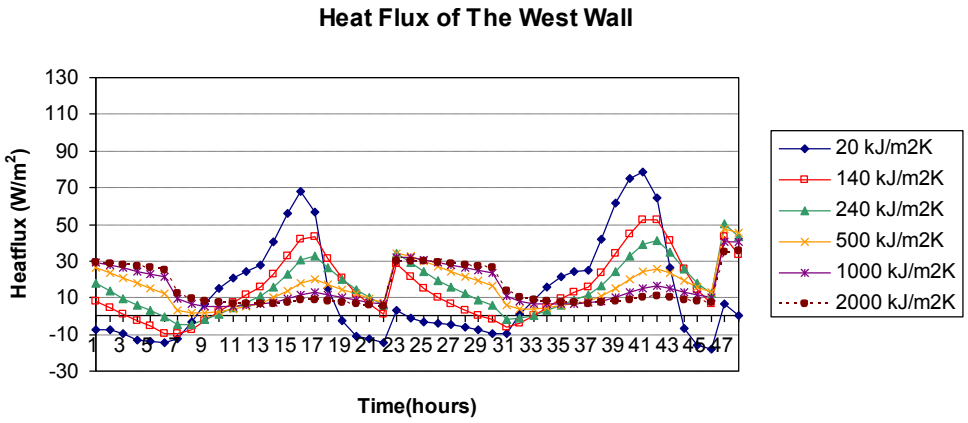

(a)

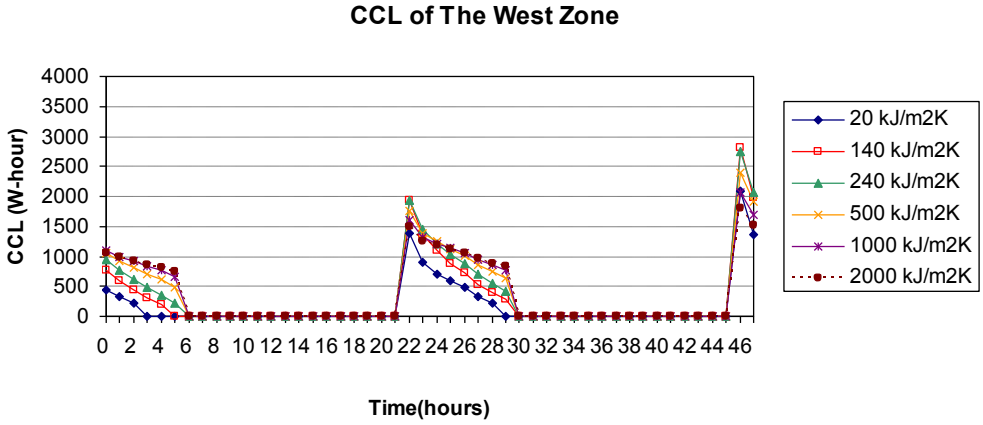

(b)

Fig. 4.15 Heat fluxes flow through the west wall and the CCL of the west zone on 28 May – 29 May

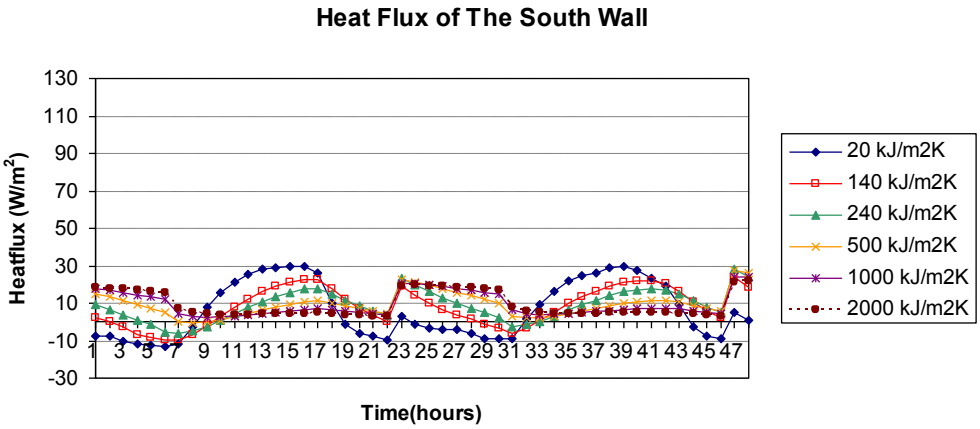

(a)

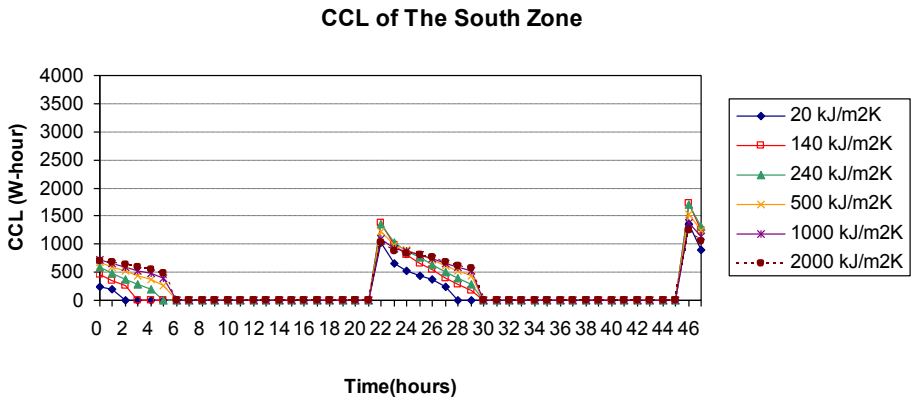

(b)

Fig. 4.16 Heat fluxes flow through the south wall and the CCL of the south zone on 28 May – 29 May.

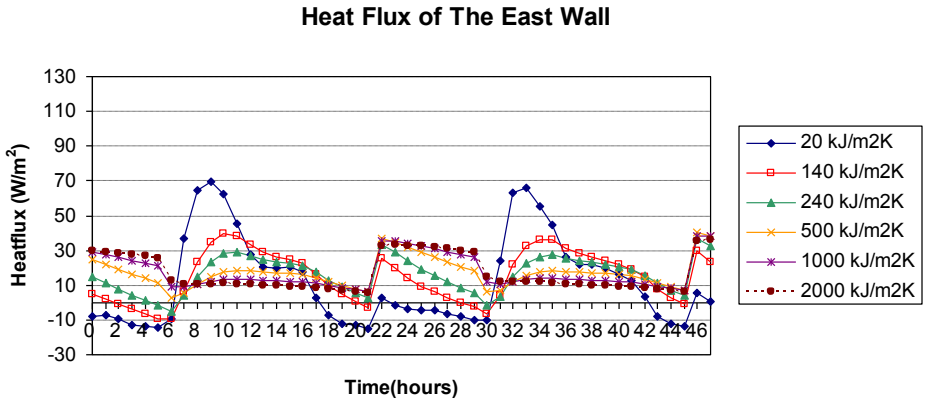

(a)

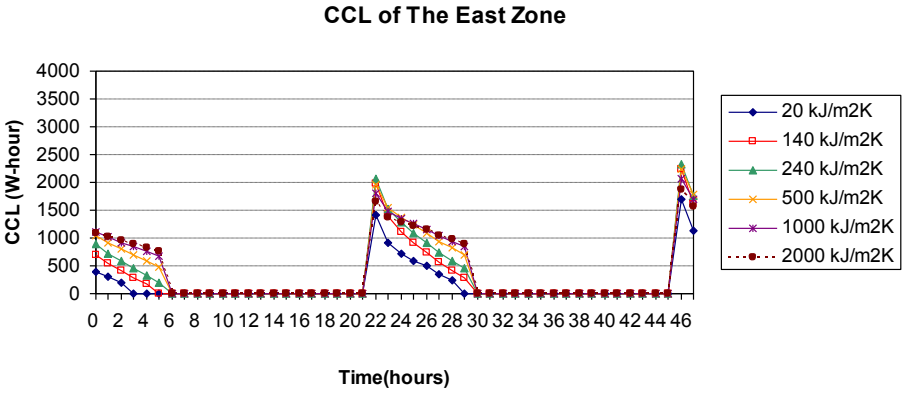

(b)

Fig. 4.17 Heat flux through the wall in an easterly direction, and CCL of the east zone on 28 May – 29 May.

The results of the annual CCL in each direction are shown in Fig.4.14- Fig 4.17. The results of this case are contrary to in the day time results. The values of annual CCL in every zone increases when the thermal mass value of the test wall increases. They are close to each other at the beginning and then the annual CCL of the north zone is clearly lower than the others. The annual CCL increases sharply when the value of thermal mass increases from 20 kJ/m^{2}K to 400 kJ/m^{2}K. For 400 kJ/m^{2}K -1,500 kJ/m^{2}K, the annual CCL in every zone shows a small increase. From these results we can conclude that small amount of thermal mass is suitable for a building operating at night.

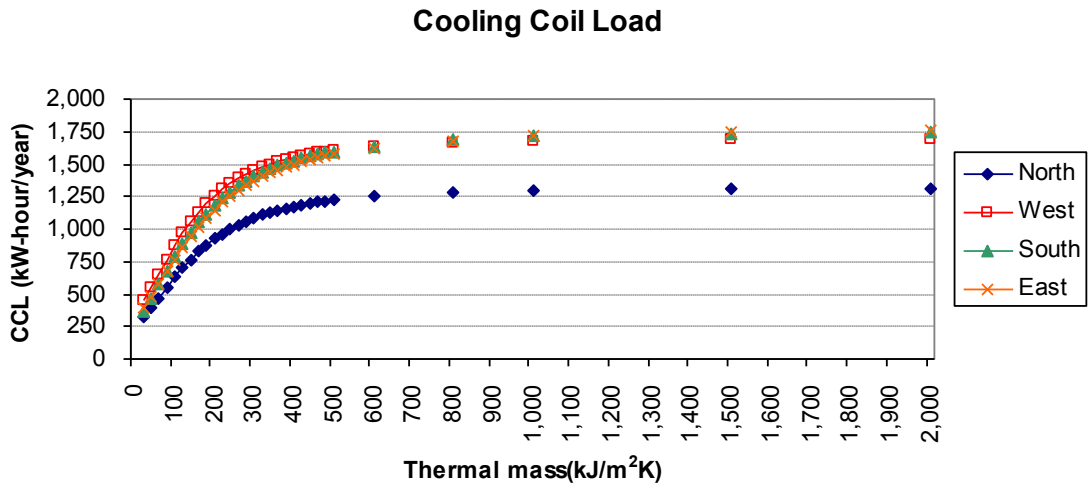

Fig.4.18 The annual CCL in each zone when the air conditioning was kept switched on at night.

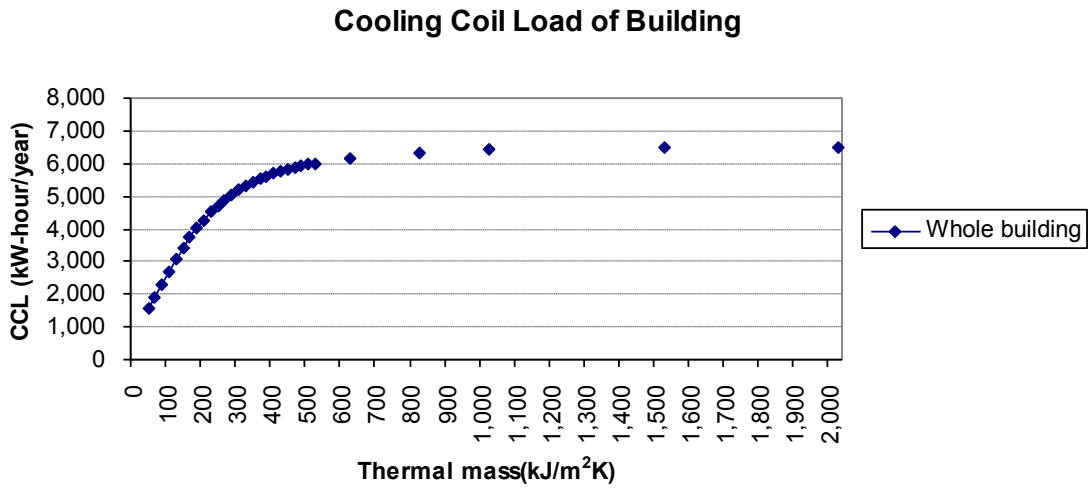

Fig.4.19 The annual CCL of the whole building when the air conditioning was kept switched on at night.

Fig.4.19 shows the annual CCL of the whole building when the air conditioner was switched on at night. The annual CCL increases when the value of thermal mass increases. The annual CCL increased sharply when the thermal mass increased from 20 kJ/m^{2}K to 400 kJ/m^{2}K. For 400 kJ/m^{2}K -2,000 kJ/m^{2}K, the CCL in every zone showed a small increase.

4.2.4 Operating time period over 24 hours, every day.

4.2.5

The operation time period of air conditioner in building in this case is assumed 24 hours, every day.

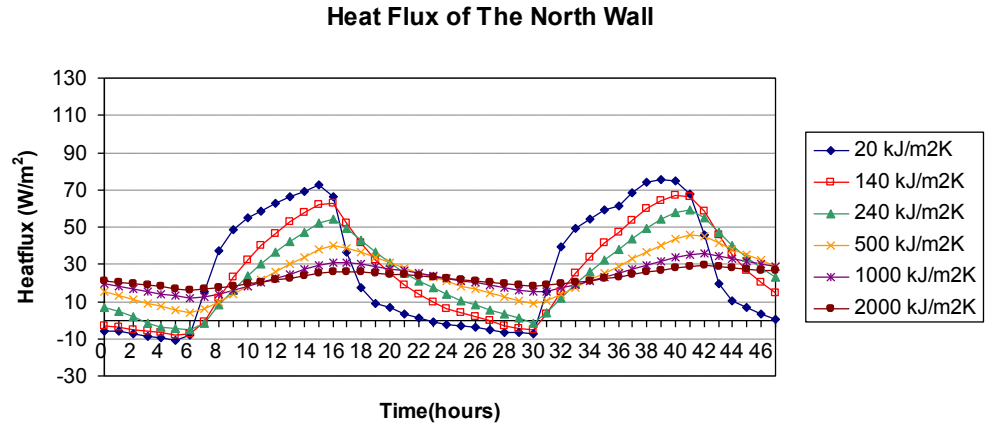

(a)

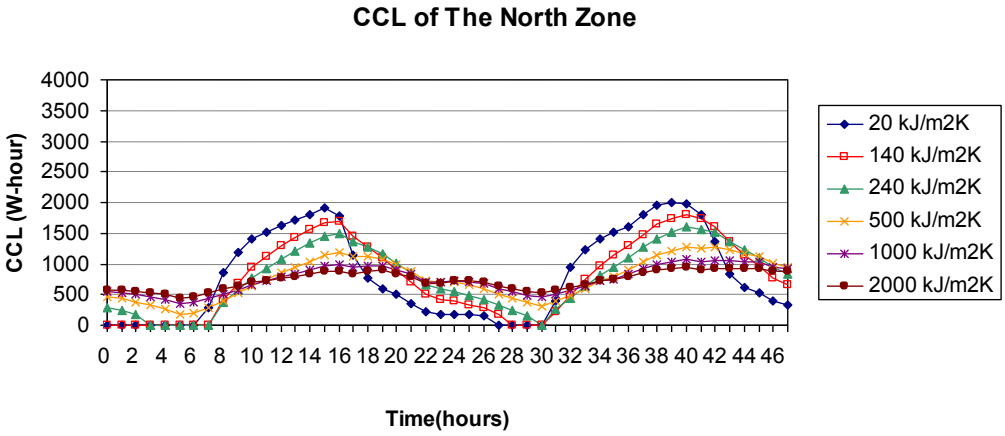

(b)

Fig. 4.20 Heat flux flow through the north wall and the CCL of the north zone on 28 May – 29 May

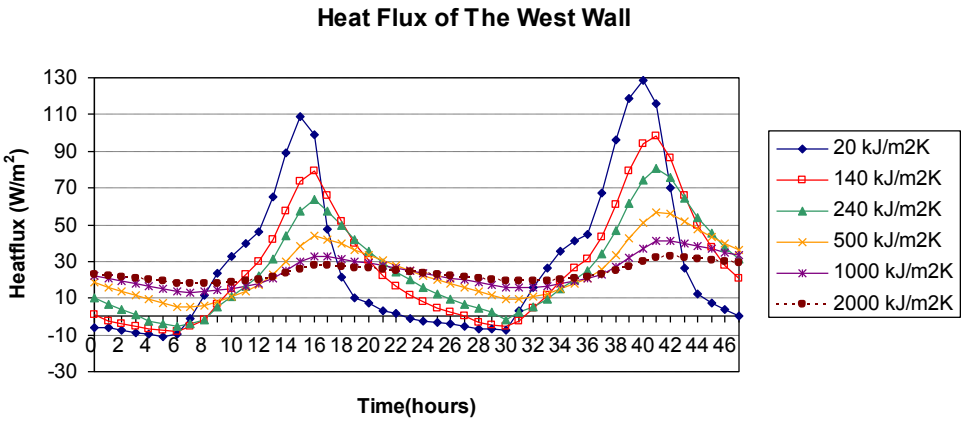

(a)

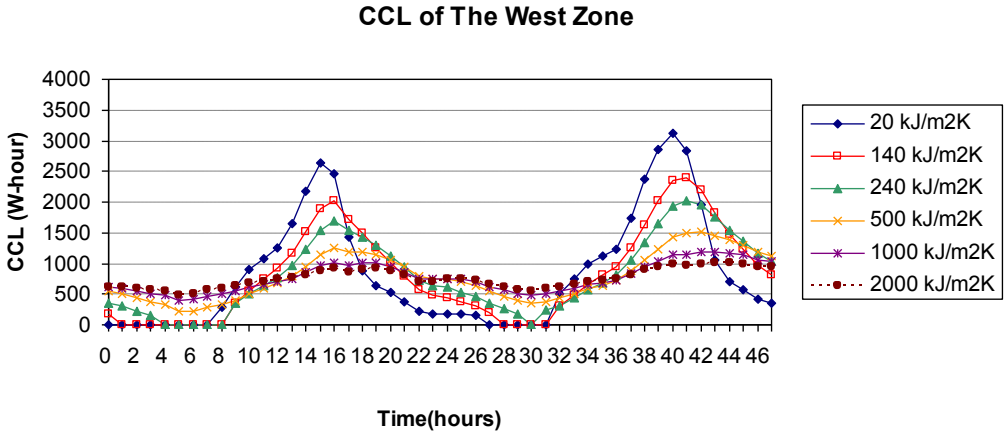

(b)

Fig. 4.21 Heat flux flow through the west wall and the CCL of the west zone on 28 May – 29 May

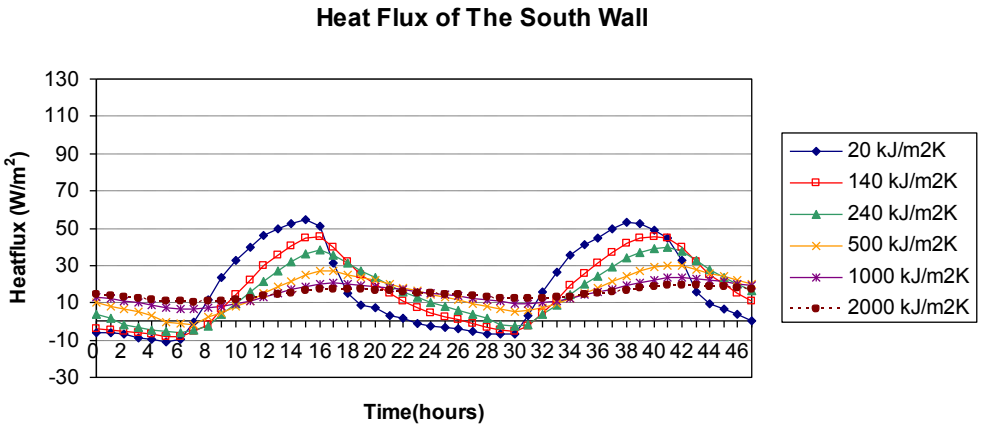

(a)

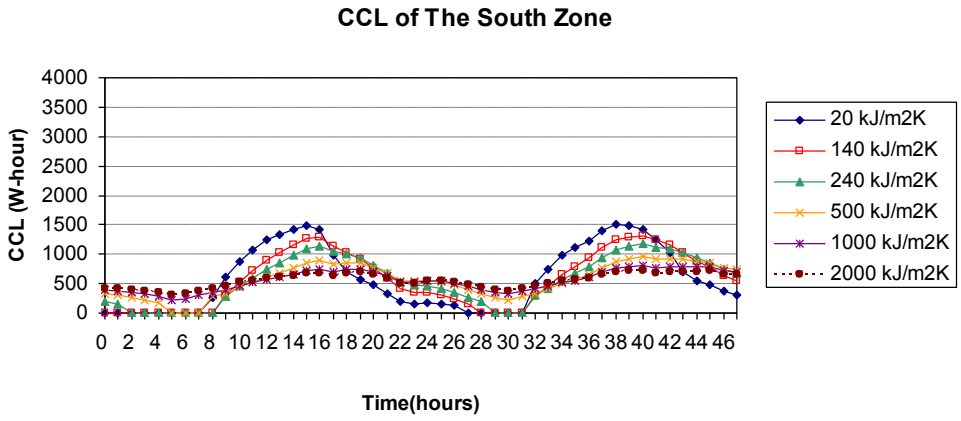

(b)

Fig. 4.22 Heat flux flow through the south wall and the CCL of the south zone on 28 May – 29 May.

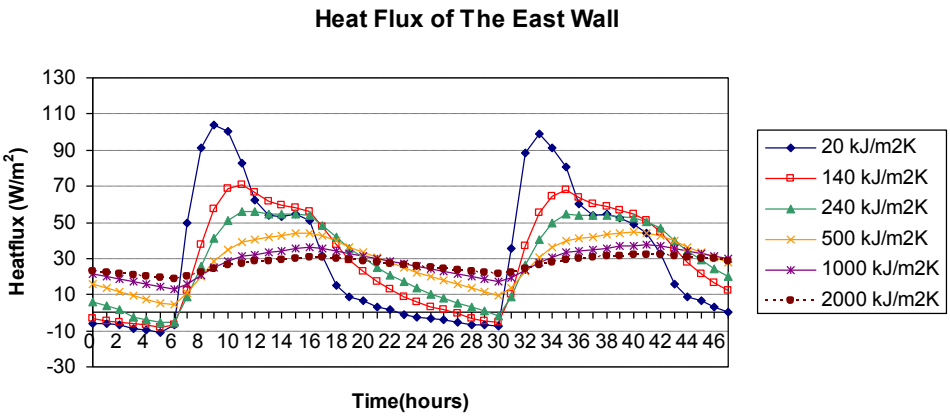

(a)

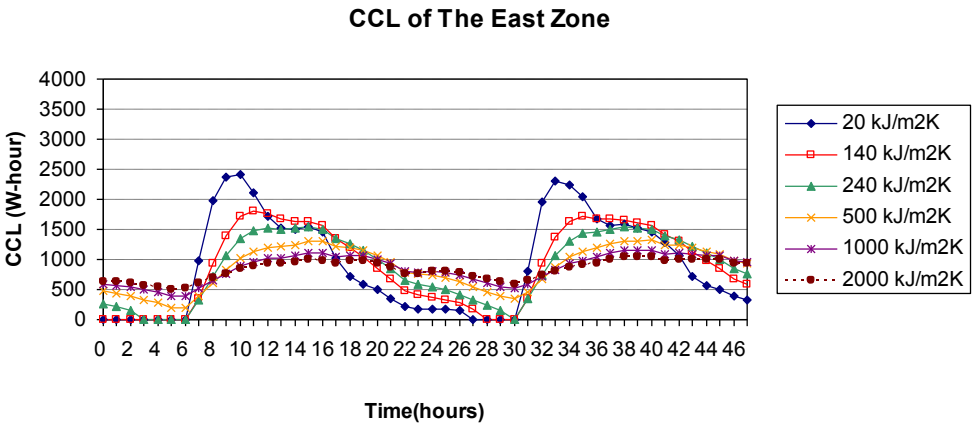

(b)

Fig. 4.23 Heat flux flow through the east wall and the CCL of the east zone on 28 May – 29 May.

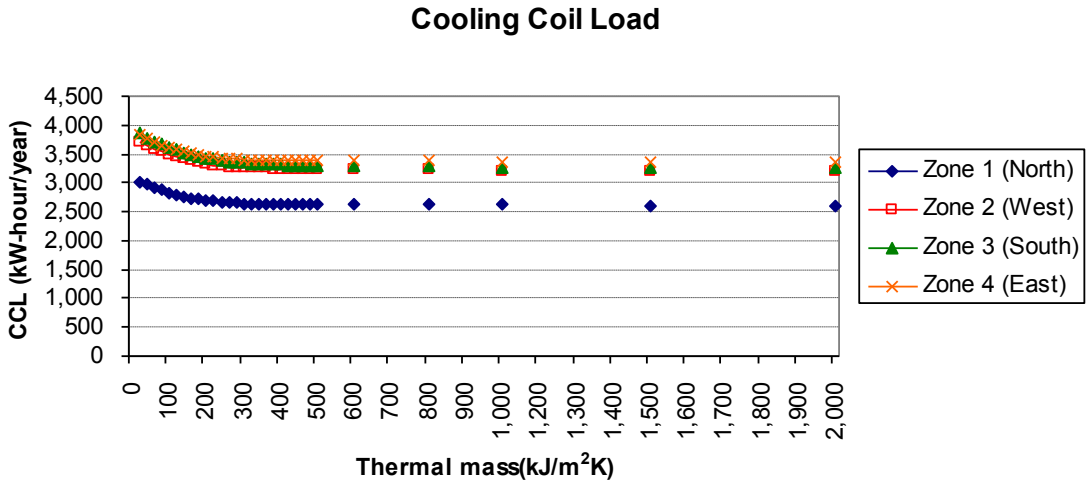

Fig.4.24 The annual CCL when keeping the air conditioner on 24 hours, every day.

Fig.4.24 shows the annual CCL of the north zone. It is obviously lower than the other zones, and the CCL of zones 2, 3 and 4 are very similar to each other. The annual CCL in every zone decreases when the thermal mass value of the test wall increases. The CCL is clearly reduced when the thermal mass increases from 20 kJ/m^{2}K to 300 kJ/m^{2}K. The annual CCL in every zone shows a small reduction when the thermal mass is greater than 300 kJ/m^{2}K. When compared to the annual CCL of 20 kJ/m^{2}K and the thermal mass of 300 kJ/m^{2}K, the CCL decreases 12.27%, 11.97%, 13.13% and 11.27 % for the north, west, south and east zones, respectively. The percentage of CCL reduction of the south wall is the highest while the east wall is the lowest.

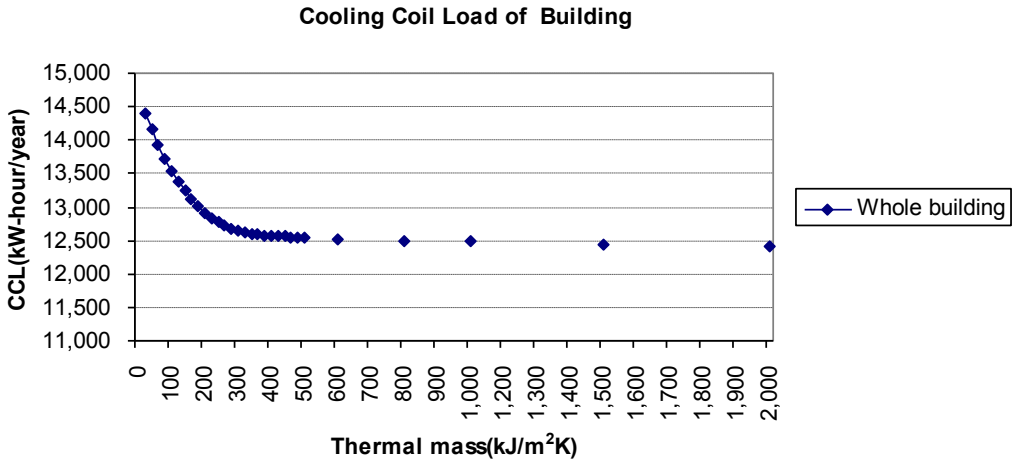

Fig.4.25 The annual CCL of the whole building when keeping the air conditioner on 24 hours

Fig.4.25 shows the CCL of the building. The CCL decreases clearly for thermal mass from 20 kJ/m^{2}K to 300 kJ/m^{2}K, and then the annual CCL show a small reduction when the value of thermal mass increases. For 300 kJ/m^{2}K thermal mass, the annual CCL is reduced by 12.16%, when compared to the annual CCL of the 20 kJ/m^{2}K thermal mass.

4.3 Results of finding the optimal thermal mass under different *WWR*

The simulation was performed on three *WWR* (0.25, 0.50 and 0.75). The study was still based on the operating time and the directions of the buildings. The annual CCL is the main criterion for evaluating the significant thermal mass. The study is focused on the value of thermal mass which has a significant influence on the CCL of the building.

4.3.1 Operating time periods in the daytime

The results of the simulation for daytime operating periods are shown in Fig.4.26. The values of annual CCL increase when *WWR* is increased because the solar radiation entering the room is greater when the *WWR* increases. The south zone and the east zone have the highest annual CCL and the north zone has the lowest annual CCL. The slope of the annual CCL graph is flatter when the value of *WWR* increases. The annual CCL reduction from increasing mass has a lower value when *WWR* increases. It indicates that the effectiveness of thermal mass, for CCL reduction decreases, when the value of *WWR* increases.

The 200 kJ/m^{2}K thermal mass is suitable for 0.25 and 0.50 *WWR*. Increasing the thermal mass has a small effect on the annual CCL reduction for 0.75 *WWR*.

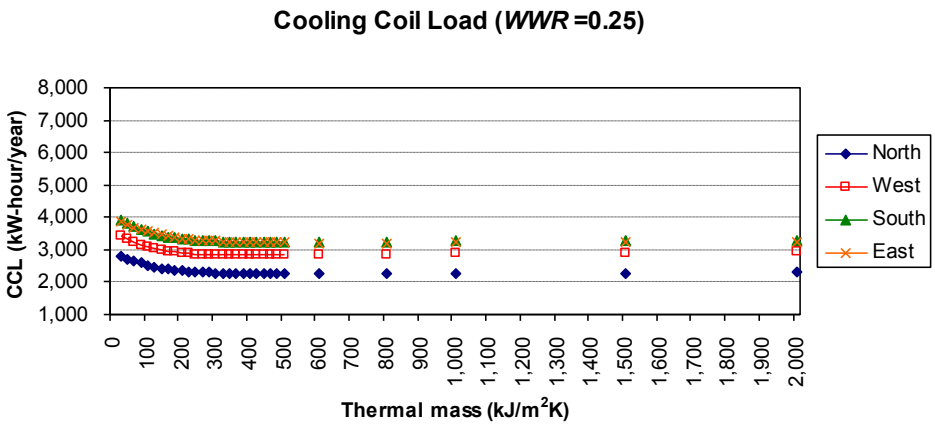

(a)

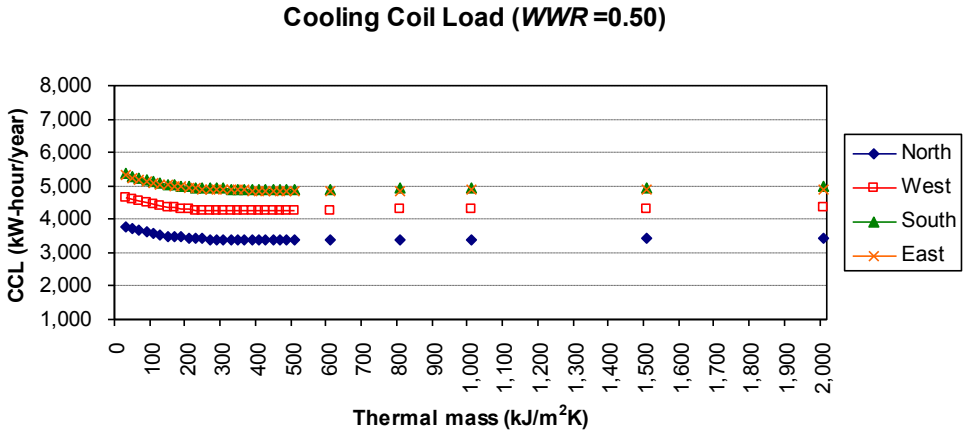

(b)

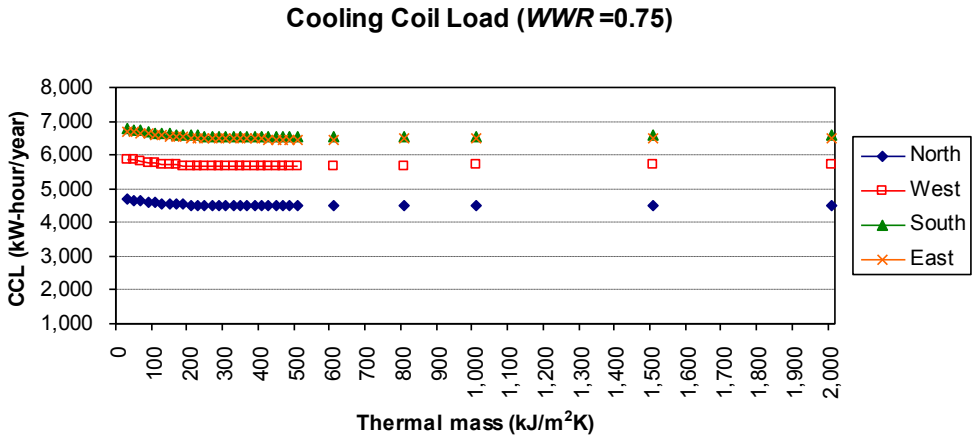

(c)

Fig. 4.26 The annual CCL in operation in the daytime , (a) *WWR*=0.25, (b) *WWR*=0.50, (c) *WWR*=0.75

The results of simulations for daytime operating periods are summarized and shown in Table 4.3 – Table 4.5.

Table 4.3 The results of simulations for daytime (WWR=0.25)

		Building	Orientation			
			North	West	South	East
1	CCLmax (kWh/year)	13,966.23	2,789.61	3,429.81	3,894.99	3,851.82
	Thermal mass (kJ/m^{2}K)	20.00	20.00	20.00	20.00	20.00
2	CCLmin (kWh/year)	11,542.35	2,259.58	2,832.89	3,234.31	3,208.
	Thermal mass (kJ/m^{2}K)	500.00	500.00	420.00	480-500	600.00
3	Suitable thermal mass(kJ/m^{2}K)	200.00	200.00	200.00	200.00	200.00
	CCL (kWh/year)	11,943.30	2,350.43	2,901.35	3,342.19	3,349.33
	CCL's reduction (%)*	14.48	15.74	15.41	14.19	13.05

Table 4.4 The results of simulations for daytime (WWR=0.50)

		Building	Orientation			
			North	West	South	East
1	CCLmax (kWh/year)	19,098.33	3,761.39	4,668.63	5,363.57	5,304.72
	Thermal mass (kJ/m^{2}K)	20.00	20.00	20.00	20.00	20.00
2	CCLmin (kWh/year)	17,383.99	3,374.86	4,249.99	4,900.77	4,853.66
	Thermal mass (kJ/m^{2}K)	460.00	480.00	380.00	460.00	500.00
3	Suitable thermal mass(kJ/m^{2}K)	200.00	200.00	200.00	200.00	200.00
	CCL (kWh/year)	17,646.85	3,438.44	4,292.55	4,970.35	4,945.51
	CCL's reduction (%)*	7.60	8.59	8.06	7.33	6.77

Table 4.5 The results of simulations for daytime (WWR=0.75)

		Building	Orientation			
			North	West	South	East
1	CCLmax (kWh/year)	24,077.19	4,696.71	5,881.19	6,788.72	6,710.57
	Thermal mass (kJ/m^{2}K)	20.00	20.00	20.00	20.00	20.00
2	CCLmin (kWh/year)	23154.69	4,487.88	5,657.94	6,538.72	6,466
	Thermal mass (kJ/m^{2}K)	420 - 440	440.00	340.00	420.00	460 - 500
3	Suitable thermal mass(kJ/m^{2}K)	100 - 200	100 - 200	100 - 200	100 - 200	100 - 200
	CCL (kWh/year)					
	CCL's reduction (%)*	1.96-3.27	2.23-3.75	2.19-3.43	1.18-3.14	1.67-2.92

*CCL's reduction, compare to CCL of 20 kJ/m^{2}K

4.3.2 Operating time periods in the evening and during the daytime

The results of simulations for evening operating periods are shown in Fig. 4.27

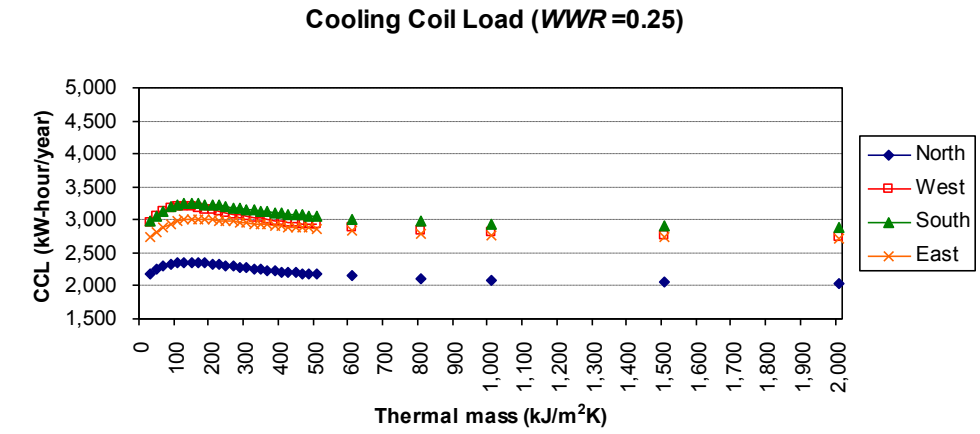

(a)

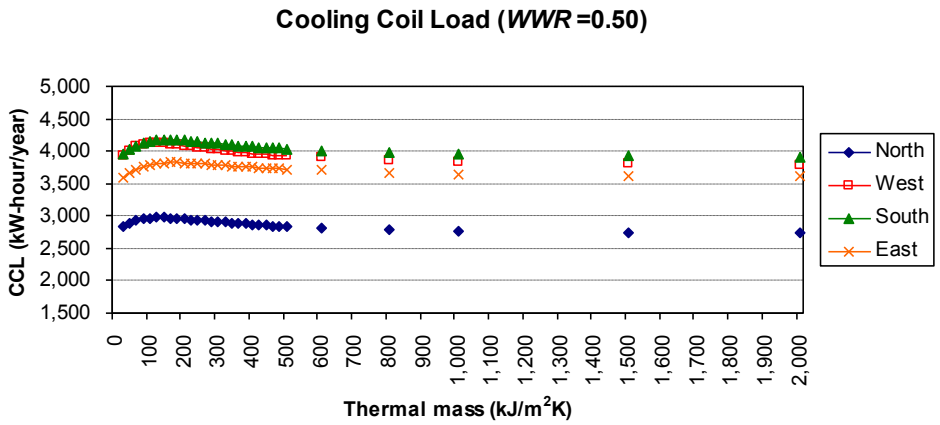

(b)

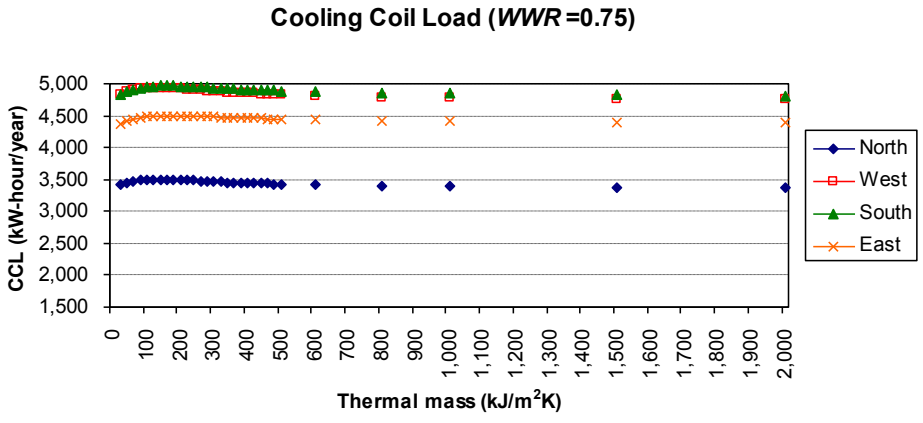

(c)

Fig. 4.27 The CCL in operation in the evening , (a) *WWR*=0.25, (b) *WWR*=0.50, (c) *WWR*=0.75

The results of simulations in the evening and during the daytime operating period are summarized and shown in Table 4.6- 4.8.

Table 4.6 The results of simulations in the evening (*WWR*=0.25)

		Building	Orientation			
			North	West	South	East
1	CCLmax (kWh/year)	11,808.37	2,359.42	3,198.90	3,247.12	3,010.98
	Thermal mass (kJ/m^{2}K)	140.00	120.00	120.00	140.00	160.00
2	CCLmin (kWh/year)	10,379.40	2,033.45	2,748.80	2,880.80	2,716.35
	Thermal mass (kJ/m^{2}K)	2,000.00	2,000.00	2,000.00	2,000.00	2,000.00
3	Suitable thermal mass(kJ/m^{2}K)	small	small	small	small	small
	CCL (kWh/year)					
	CCL's reduction (%)					

Table 4.7 The results of simulations in the evening (WWR=0.50)

		Building	Orientation			
			North	West	South	East
1	CCLmax (kWh/year)	15,083.24	2,973.14	4,122.13	4,174.15	3,822.12
	Thermal mass (kJ/m^{2}K)	140.00	120.00	120.00	140.00	180.00
2	CCLmin (kWh/year)	14,039.48	2,731.74	3,790.42	3,908.17	3,609.16
	Thermal mass (kJ/m^{2}K)	2,000.00	2,000.00	2,000.00	2,000.00	20.00
3	Optimal thermal mass(kJ/m^{2}K)	small	small	small	small	small
	CCL (kWh/year)					
	CCL's reduction (%)					

Table 4.8 The results of simulations in the evening (WWR=0.75)

		Building	Orientation			
			North	West	South	East
1	CCLmax (kWh/year)	17,904.20	3,503	4,936.99	4,967	4,500.29
	Thermal mass (kJ/m^{2}K)	140.00	120 -140	120.00	140 - 160	180.00
2	CCLmin (kWh/year)	17,320.28	3,369.57	4,751.30	4,817.00	4,367.22
	Thermal mass (kJ/m^{2}K)	2,000.00	2,000.00	2,000.00	2,000.00	20.00
3	Optimal thermal mass(kJ/m^{2}K)	small	small	small	small	small
	CCL (kWh/year)					
	CCL's reduction (%)					

4.3.3 Operating time periods at night

The results of simulation for night operation periods are shown below.

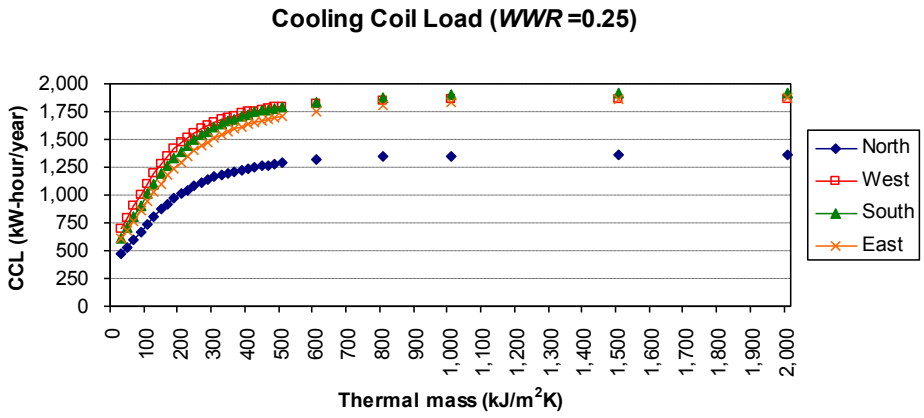

(a)

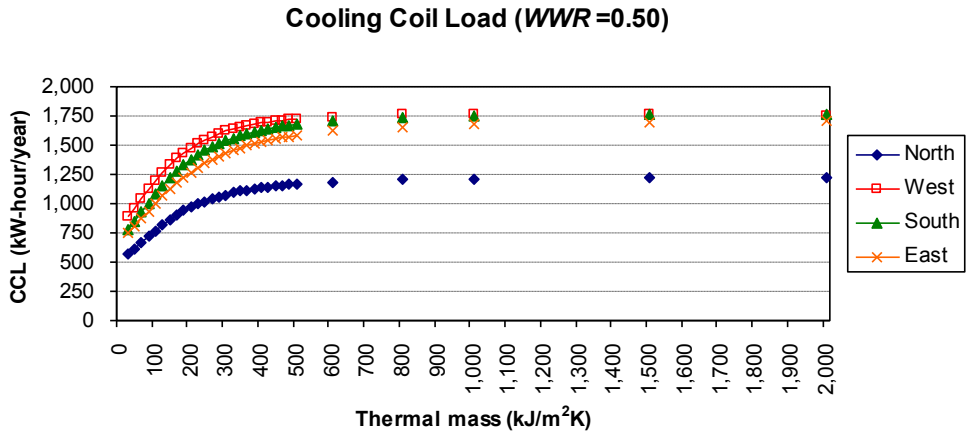

(b)

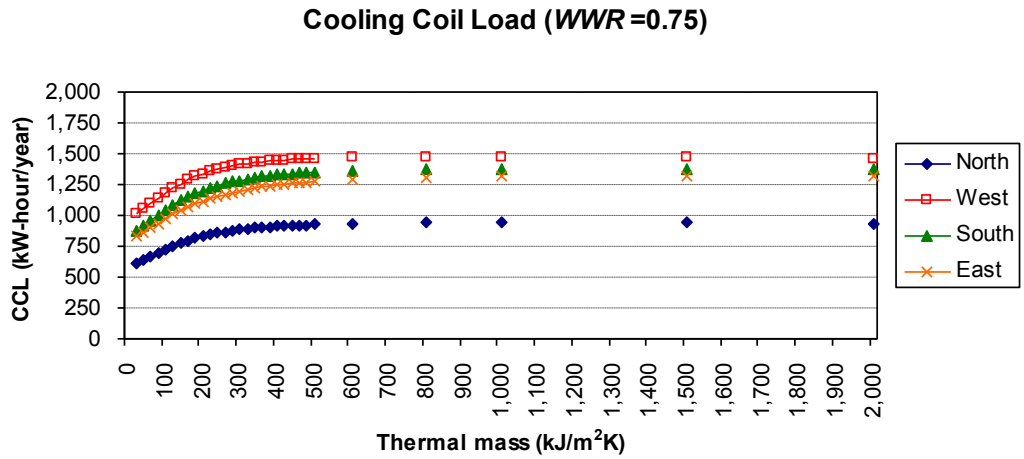

(c)

Fig. 4.28 The CCL in operation at night, (a) *WWR*=0.25, (b) *WWR*=0.50, (c) *WWR*=0.75

The results of simulations for night operation periods are summarized and shown in Table 4.9-Table 11.

Table 4.9 The results of simulations for night operations (WWR=0.25)

		Building	Orientation			
			North	West	South	East
1	CCLmax (kWh/year)	7,023.89	1,363.66	1,864.59	1,922.60	1,875.90
	Thermal mass (kJ/m^{2}K)	2,000.00	2,000.00	1,500.00	2,000.00	2,000.00
2	CCLmin (kWh/year)	2,387.25	469.54	701.25	612.28	604.18
	Thermal mass (kJ/m^{2}K)	20.00	20.00	20.00	20.00	20.00
3	Suitable thermal mass(kJ/m^{2}K)	small	small	small	small	small
	CCL (kWh/year)					
	CCL's reduction (%)					

Table 4.10 The results of simulations for night operations (WWR=0.50)

		Building	Orientation			
			North	West	South	East
1	CCLmax (kWh/year)	6,441.17	1,220.87	1,763.29	1,763.43	1,701.87
	Thermal mass (kJ/m^{2}K)	1,500.00	1,500.00	1,000.00	1,500.00	2,000.00
2	CCLmin (kWh/year)	2,978.94	564.70	890.63	773.45	750.15
	Thermal mass (kJ/m^{2}K)	20.00	20.00	20.00	20.00	20.00
3	Suitable thermal mass(kJ/m^{2}K)	small	small	small	small	small
	CCL (kWh/year)					
	CCL's reduction (%)					

Table 4.11 The results of simulations for night operations (WWR=0.75)

		Building	Orientation			
			North	West	South	East
1	CCLmax (kWh/year)	3,110.89	546.47	936.38	819.03	812.42
	Thermal mass (kJ/m^{2}K)	800.00	800.00	800.00	600.00	1,000.00
2	CCLmin (kWh/year)	2,060.45	361.39	652.42	524.68	521.96
	Thermal mass (kJ/m^{2}K)	20.00	20.00	20.00	20.00	20.00
3	Suitable thermal mass(kJ/m^{2}K)	small	small	small	small	small
	CCL (kWh/year)					
	CCL's reduction (%)					

4.3.4 Operating time periods over 24 hours

The results of simulations for 24 hour operating periods are shown below.

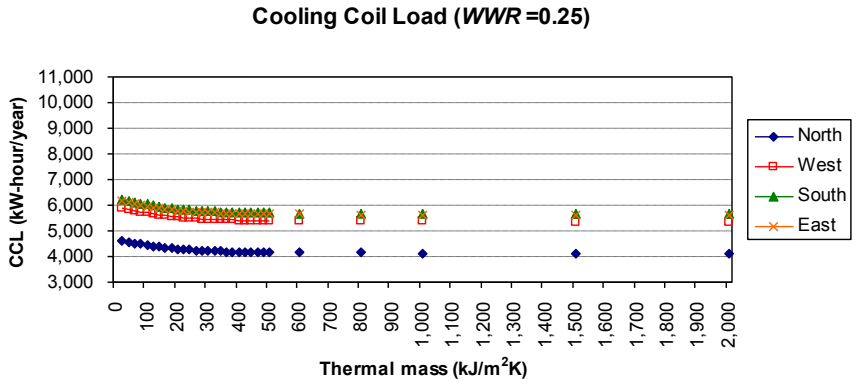

(a)

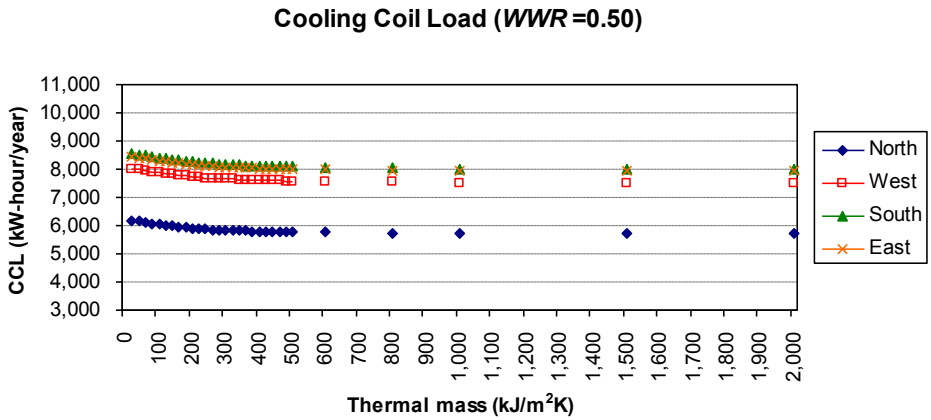

(b)

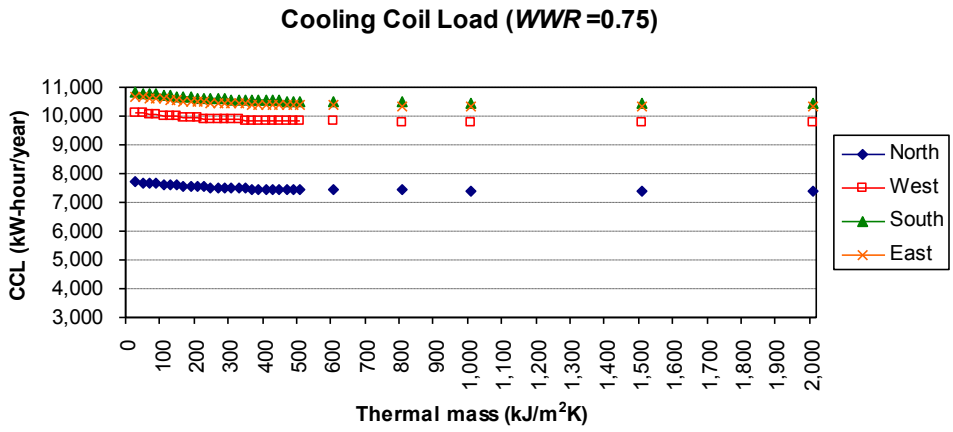

(c)

Fig.4.29 The CCL in operation for 24 hours , (a) *WWR*=0.25, (b) *WWR*=0.50, (c) *WWR*=0.75.

The results of simulations for 24 hour operating periods are summarized and shown in Table 4.12 – Table 4.14.

Table 4.12 The results of simulations for 24 hour operations (WWR=0.25)

		Building	Orientation			
			North	West	South	East
1	CCLmax (kWh/year)	22,896.05	4,612.97	5,885.29	6,239.73	6,158.07
	Thermal mass (kJ/m^{2}K)	20.00	20.00	20.00	20.00	20.00
2	CCLmin (kWh/year)	20,719.32	4,115.49	5,342.51	5,649.14	5,612.18
	Thermal mass (kJ/m^{2}K)	2,000.00	2,000.00	2,000.00	2,000.00	2,000.00
3	Suitable thermal mass(kJ/m^{2}K)	200-300	200-300	200-300	200-300	200-300
	CCL (kWh/year)	21,141.50	4,215.47	5,452.25	5,768.51	5,705.27
	CCL's reduction (%)	7.66	8.62	7.36	7.55	7.35

Table 4.13 The results of simulations for 24 hour operations (WWR=0.50)

		Building	Orientation			
			North	West	South	East
1	CCLmax (kWh/year)	31,237.83	6,193.72	8,020.49	8,566.89	8,456.74
	Thermal mass (kJ/m^{2}K)	20.00	20.00	20.00	20.00	20.00
2	CCLmin (kWh/year)	29,108.64	5,698.41	7,495.94	7,990.71	7,923.59
	Thermal mass (kJ/m^{2}K)	2,000.00	2,000.00	2,000.00	2,000.00	2,000.00
3	Suitable thermal mass(kJ/m^{2}K)	200-300	200-300	200-300	200-300	200-300
	CCL (kWh/year)	29,723.52	5,836.78	7,651.62	8,166.82	8,068.29
	CCL's reduction (%)	4.85	5.76	4.60	4.67	4.59

Table 4.14 The results of simulations for 24 hour operations (WWR=0.75)

		Building	Orientation			
			North	West	South	East
1	CCLmax (kWh/year)	30,323.94	5,713.11	7,845.62	8,441.85	8,323.35
	Thermal mass (kJ/m^{2}K)	20.00	20.00	20.00	20.00	20.00
2	CCLmin (kWh/year)	29,042.41	5,415.10	7,524.14	8,101.13	8,002.04
	Thermal mass (kJ/m^{2}K)	2,000.00	2,000.00	2,000.00	2,000.00	2,000.00
3	Suitable thermal mass(kJ/m^{2}K)	200-300	200-300	200-300	200-300	200-300
	CCL (kWh/year)					
	CCL's reduction (%)	1.86-2.42	2.24-2.89	1.73-2.27	1.77-2.33	1.78-2.30

4.4 Results of evaluations of the insulation position of the massive wall configurations.

In this section, the results of the parameters, the operating time periods and the sequence of materials, were discussed. The analyses were conducted for wall configurations that were mentioned in the previous chapter and for the cardinal directions.

4.4.1 Operating time periods in daytime

The results of simulations during the daytime operating periods are shown in Fig.2.49. The cooling coil load in zones 1-4 were simulated as a function of the position of insulation of the test wall. The operating time periods of the air conditioners in buildings were assumed to be from 8:00 a.m. until 5:00 p.m. on weekdays.

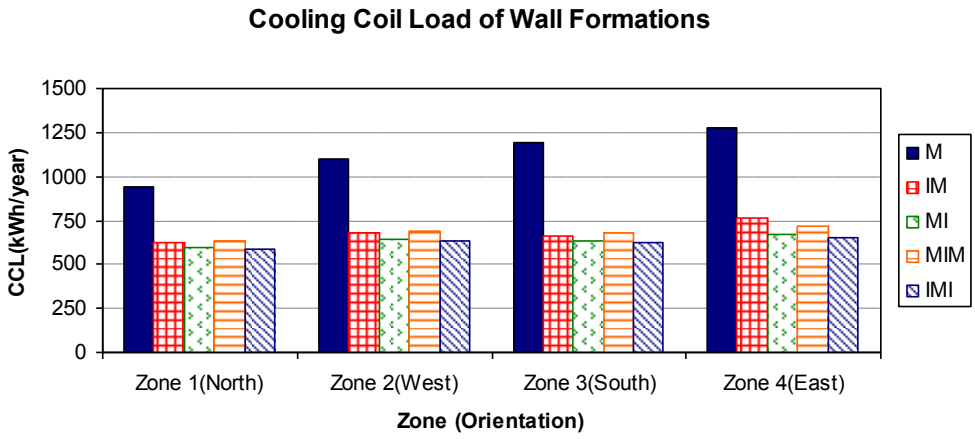

Fig.4.30 The annual CCL of the wall formations when keeping the air conditioners on during the daytime, opaque wall (*WWR*=0).

For the opaque wall case, zone 1, the test wall faces north, and the annual CCL of the M wall was at 945.25 kWh/year. For the insulated walls, the maximum CCL wall was the MIM, at 637.30 kWh/year, and the minimum CCL wall was the IMI at 584.75 kWh/year. In zone 2, the test wall faces west, and the annual CCL of the M wall was at 1,096.22 kWh/year. For the insulated walls, the maximum CCL wall was the MIM, at 693.82 kWh/year, and the minimum CCL wall was the IMI at 634.23 kWh/year. In zone 3, the test wall faces south, the CCL of the M wall was at 1,196.08 kWh/year. For the insulated walls, the maximum CCL wall was the MIM, at 681.46 kWh/year and the minimum CCL wall was the IMI, at 619.85 kWh/year. In zone 4, the test wall faces east, the CCL of the M

wall was at 1,273.18 kWh/year. For the insulated walls, the maximum CCL wall was the IM, at 766.03 kWh/year and the minimum CCL was the IMI wall at 652.19 kWh/year.

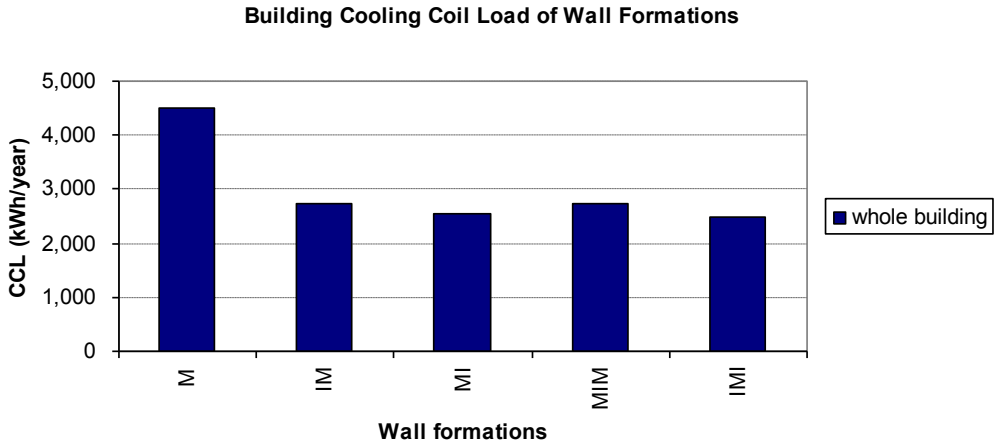

Fig.4.31 Building cooling coil load of wall formations, daytime, opaque wall (*WWR*=0).

Fig.4.31 shows the building's CCL, plus the totals of the CCL in every zone. The M wall's CCL was 4,510.73 kWh/year. For the insulated walls, the IM wall was the wall formation which had the maximum CCL at 2,735.17 kWh/year followed by the MIM and MI at 2,726.88 kWh/year and 2,550.28 kWh/year, respectively. The IMI wall had the minimum CCL at 2,491.02 kWh/year.

In terms of the annual CCL reductions, when compared to the annual CCL of the M wall, IMI wall had the greatest CCL reduction at 44.78% followed by MI, MIM and IM at 43.46%, 39.55% and 39.36%, respectively. As the results indicated, the position of insulation has a small effect on the CCL reduction for massive wall.

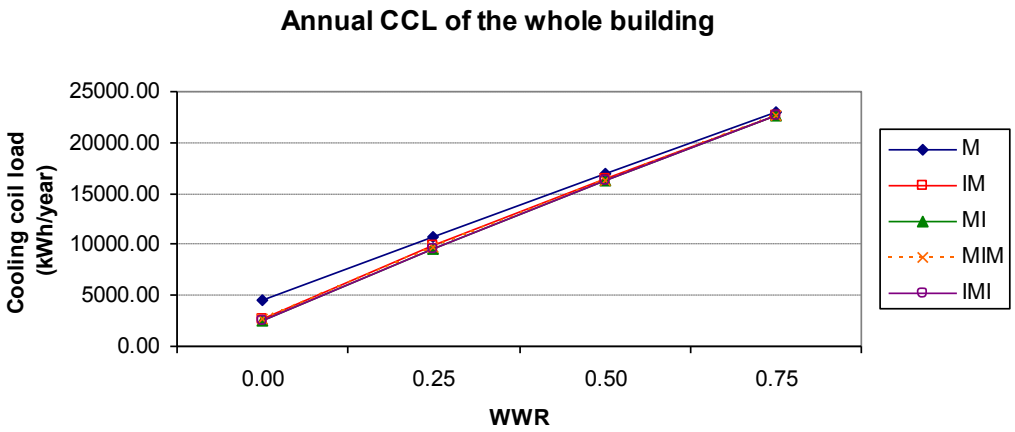

Fig.4.32 Building CCL of wall formations under different *WWR* during daytime operation.

Fig.4.32 shows the relationship between the annual CCL of building and the *WWR*. The annual CCL increased when there was a higher *WWR*. The annual CCL of the insulated walls were clearly lower than the M wall type for opaque walls (*WWR* = 0), but they were more similar to the M wall when the value of the *WWR* increased. It indicated that the influence of insulation is reduced when *WWR* is increased for massive walls, and the position of insulation has a small effect on the annual CCL reduction for massive walls.

4.4.2 Operating time periods in the evening and during the daytime

The results of simulations for daytime and evening operating periods are shown in Fig.4.33. The operating time periods of the air conditioners in the building was assumed to be from 6:00 p.m. until 10:00 p.m. on weekdays and from 10 a.m. until 10:00 p.m. at the weekend.

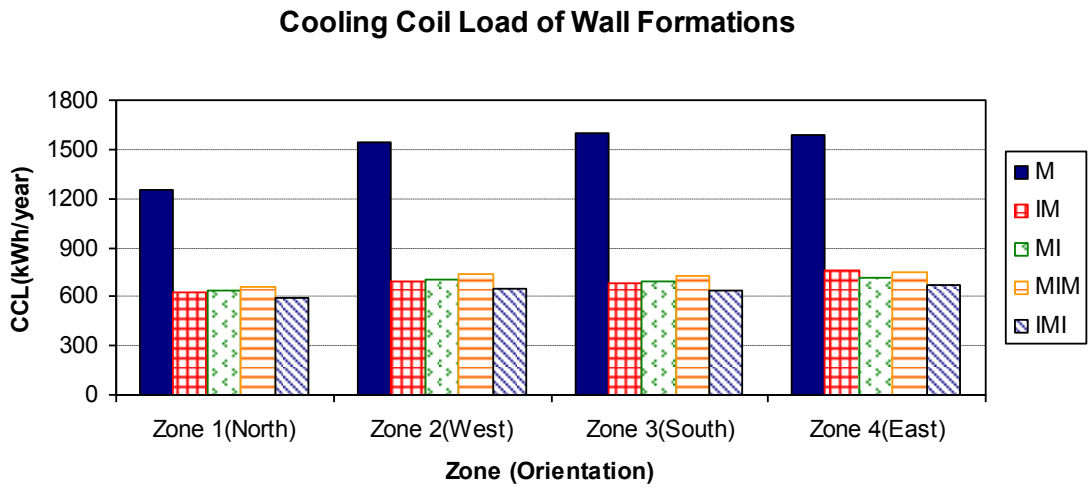

Fig.4.33 The annual CCL of the wall formations when keeping the air conditioning on during the daytime and evening

In zone 1, the test wall faces north, the annual CCL of the M wall is 1,248.99 kWh/year. For the insulated walls, the maximum CCL wall was the MIM , 661.96 kWh/year, and the minimum CCL wall was the IMI, 590.23 kWh/year. In zone 2, the test wall faces west, the annual CCL of the M wall was 1,544.71 kWh/year. For the insulated walls, the maximum CCL wall was the MIM, 735.25 kWh/year, and the minimum CCL wall was the IMI, at 651.02 kWh/year. In zone 3, the test wall faces south, the annual CCL of the M wall was 1,594.13 kWh/year. For the insulated walls, the maximum CCL was the MIM wall, 721.65 kWh/year, and the minimum CCL wall was the IMI, 636.15 kWh/year.

In zone 4, the test wall faces east, the annual CCL of the M wall was 1,584.34 kWh/year. For the insulated walls, the maximum CCL wall was the IM, 755.85 kWh/year, and the minimum CCL wall was the IMI, 669.72 kWh/year.

Fig.4.34 shows the CCL of all the buildings, plus the totals of CCL in every zone. The M wall's CCL was 5,972.17 kWh/year. For the insulated walls, the MIM wall was the wall formation which had the maximum CCL at 2872.14 kWh/year, followed by the IM and the MI at 2766.69 kWh/year and 2737.23 kWh/year, respectively. The IMI wall was the formation which had the minimum CCL, at 2547.12 kWh/year.

In terms of the annual CCL reduction, when compared to the annual CCL of the M wall, the IMI wall had the greatest CCL reduction at 57.35% followed by the MI, IM and MIM at 54.17%, 53.67% and 51.91%, respectively. The position of insulation had little influence on the CCL changes for massive walls.

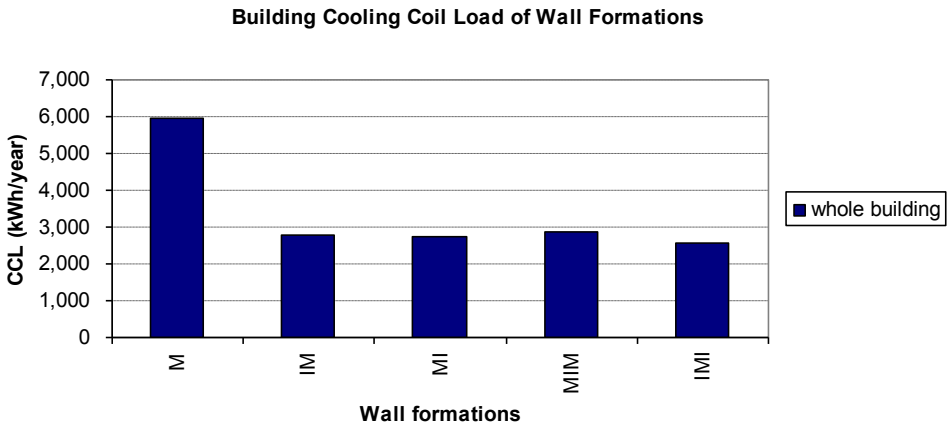

Fig.4.34 The building CCL of wall formations, in the evening and during the daytime.

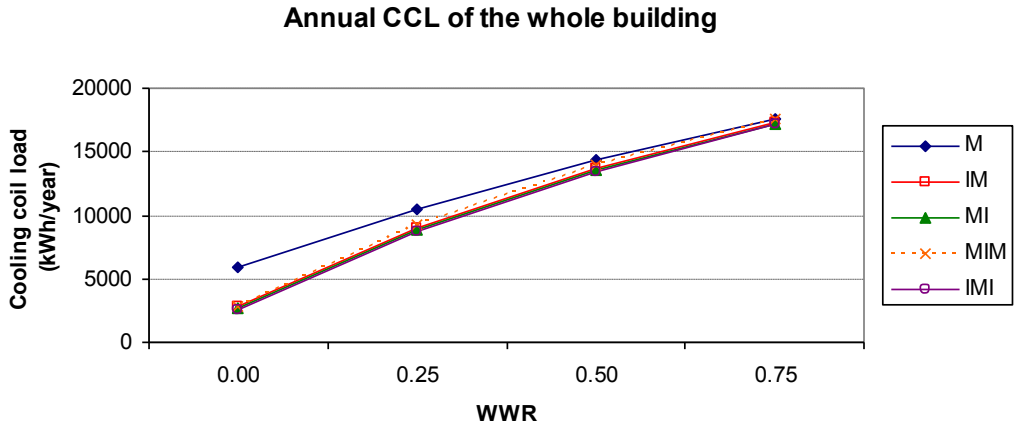

Fig.4.35 The building CCL of wall formations, under different *WWR* and daytime and evening operation.

Fig.4.35 shows the relationship between the annual CCL of building and *WWR*. The annual CCL increased when there was a higher *WWR*, but they were not similar in daytime cases, their graphs were not linear. The annual CCL of the insulated walls were clearly lower than the M wall type for an opaque wall (*WWR* = 0), but they were similar to the M wall when the value of *WWR* increased. For daytime and evening operation, the influence of insulation was reduced when *WWR* for the massive wall increased, and the position of insulation had a small effect on the annual CCL reduction for massive walls.

4.4.3 The operating time period at night

The results of simulations for daytime and evening operating periods, are shown in Fig.4.36 The operating time periods of the air conditioning in buildings was assumed to be from 10:00 p.m. until 6:00 a.m. on weekdays, and from 10:00 p.m. until 8:00 a.m. at the weekend.

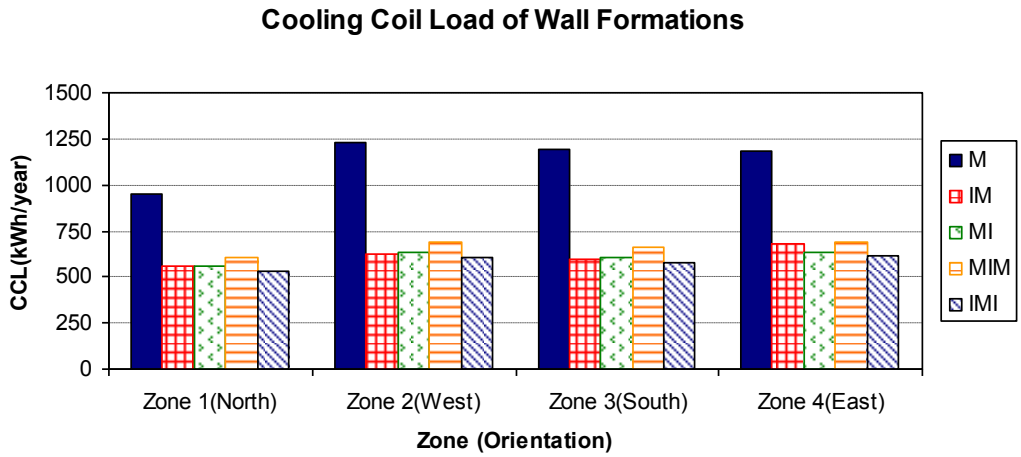

Fig.4.36 The annual CCL of the wall formations when keeping the air conditioning on at night.

In zone 1, the test wall faces north, the annual CCL of the M wall was 948.67 kWh/year. For the insulated walls, the maximum CCL wall was the MIM, at 605.50 kWh/year, and the minimum CCL wall was the IMI, at 534.83 kWh/year. In zone 2, the test wall faces west, the annual CCL of the M wall was 1,231.96 kWh/year. For the insulated walls, the maximum CCL wall was the MIM, at 689.20 kWh/year and the minimum CCL wall was the IMI, at 604.33 kWh/year. In zone 3, the test wall faces to the south, the annual CCL of M wall was 1,193.15 kWh/year. For the insulated walls, the

maximum CCL wall was MIM, at 657.62 kWh/year and the minimum CCL wall was the IMI, at 577.10 kWh/year. In zone 4, the test wall faces east, the annual CCL of the M wall was 1183.95 kWh/year. For the insulated walls, the maximum CCL wall was the MIM, at 689.64 kWh/year and the minimum CCL wall was the IMI, at 616.22 kWh/year.

Fig.4.37 shows the CCL of the buildings, plus the totals of the CCL in every zone. The M wall's CCL was 4,557.73 kWh/year. For the insulated walls, the MIM wall was the wall formation which had the maximum CCL at 2641.95 kWh/year followed by the IM and MI at 2,460.28 kWh/year and 2,440.29 kWh/year, respectively. The IMI wall was the formation which had the minimum CCL at 2,332.47 kWh/year.

In term of reduction, when compared to the annual CCL of the M wall, the IMI wall had the greatest CCL reduction at 48.82% followed by the MI, IM and MIM at 46.46%, 46.02% and 42.03%, respectively.

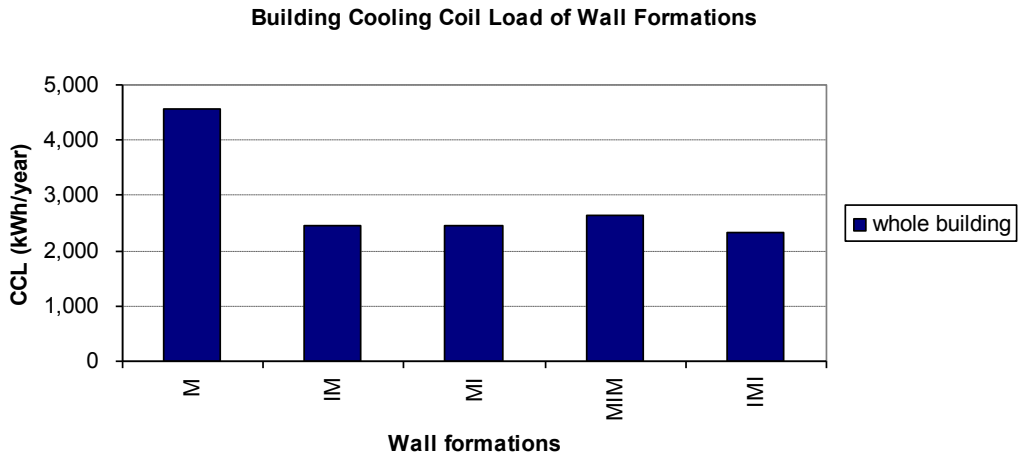

Fig.4.37 The building cooling coil loads of wall formations, at night

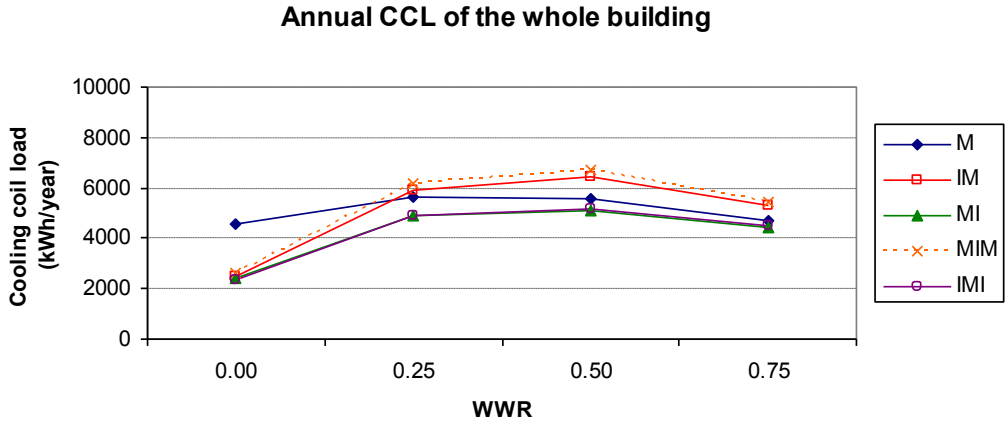

Fig.4.38 The building CCL of wall formations under different *WWR* and night operations

Fig.4.38 shows the relationship between the annual CCL of buildings and the *WWR*. The annual CCL of the insulated walls were clearly lower than the M wall types for opaque wall (*WWR* = 0), but, when WWR was 0.25, 0.50 and 0.75, the annual CCL of the IM and MIM wall was higher than the M wall. This showed that the insulated wall with an inner thermal mass caused high CCL, because the inner stored heat, from solar radiation entering through the window area, could not penetrated the insulation at night, so it was only released into the room. When considering only the insulated wall, the annual CCL of 0.25 *WWR* was lower than the annual CCL of 0.50 *WWR*. The solar radiation entering was much greater when the window area was increases and this caused higher CCL at night. But, the annual CCL of 0.50 *WWR* was lower than the annual CCL of 0.75 *WWR*. This can be explained, as follow ;

- the thermal mass area was reduced when the window area was increased, thus, the absorbed heat of 0.75 *WWR* was less than the absorbed heat of 0.50 *WWR*.
- the heat in the room flowed out through the windows more effectively than being conducted through the opaque wall at night.

From these results, it may be concluded that the IM wall and MIM wall, inner thermal mass, is unsuitable for night operation in buildings, particularly the building which has a window area.

4.3.4 Operating time period over 24 hours, every day

The results of simulations for daytime and evening operating periods are shown in Fig.4.39. The operating time period of the air conditioning in buildings assumes that the air conditioning is kept on 24 hours every day.

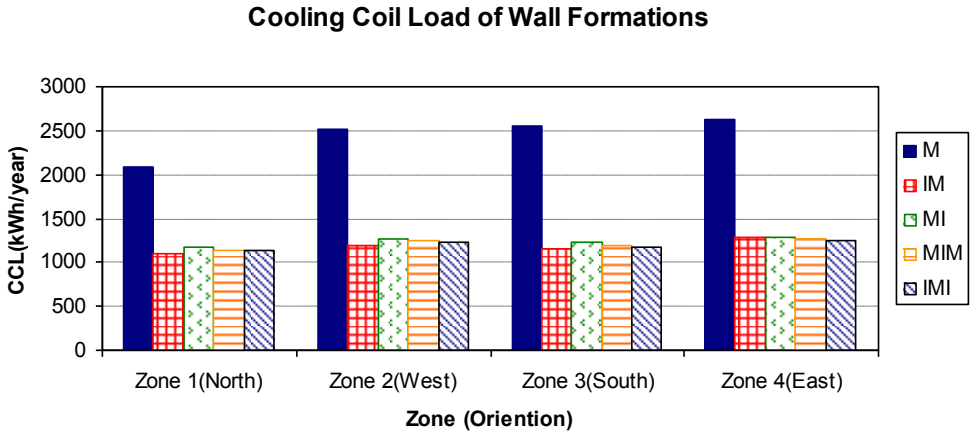

Fig.4.39 The annual CCL of the wall formations when the air conditioning is kept on 24 hours.

In zone 1, the test wall faces north, the annual CCL of the M wall was 2,078.80 kWh/year. For the insulated walls, the maximum CCL wall was the MI wall, at 1,165.85 kWh/year, and the minimum CCL wall was the IM wall, at 1100.99 kWh/year. In zone 2, the test wall faces west, the annual CCL of M wall was 2,515.12 kWh/year. For the insulated walls, the maximum CCL wall was the MI wall, at 1,266.56 kWh/year and the minimum CCL wall was the IM wall, at 1,192.71 kWh/year. In zone 3, the test wall faces south, the annual CCL of the M wall was 2,543.58 kWh/year. For the insulated walls, the maximum CCL wall was the MI wall, at 1,222.26 kWh/year, and the minimum CCL wall was the IM wall, at 1,147.60 kWh/year. In zone 4, the test wall faces east, the annual CCL of the M wall was 2,620.74 kWh/year. For the insulated walls, the maximum CCL wall was the IM wall, at 1,293.97 kWh/year, and the minimum CCL wall was IMI wall, at 1,247.86 kWh/year.

Fig.4.40 shows the CCL of the buildings, plus the totals of the CCL in every zone. The M wall's CCL is 9,758.25 kWh/year. For the insulated walls, the MI wall is the wall formation which has the maximum CCL at 4,941.14 kWh/year, followed by MIM and IMI walls at 4,849.10 kWh/year and 4,787.58 kWh/year, respectively. The IM wall was the formation which had the minimum CCL at 4,735.26 kW/year.

In terms of reductions when comparing the CCL of the M wall, the IM wall had the greatest CCL reduction at 51.47 %, followed by IMI, MIM and MI walls at 50.94%, 50.31% and 49.36%, respectively. The position of insulation had little influence on the CCL changes for the massive walls.

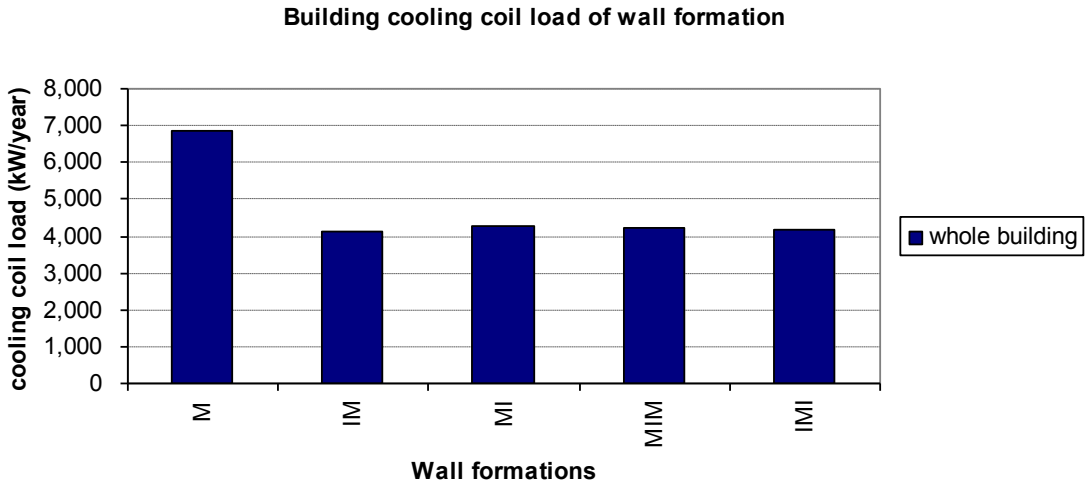

Fig.4.40 Building cooling coil load of wall formations, 24 hours

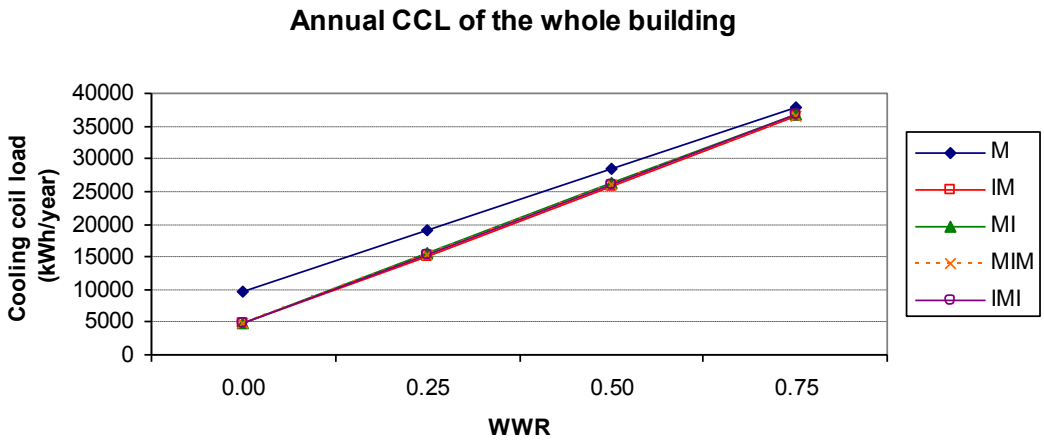

Fig.4.41 Building CCL of wall formations under different *WWR* and night operations

As shown in Fig.4.41, the annual CCL increased when the value of the *WWR* increased, the same as during the day. The annual CCL of the insulated walls were clearly lower than the M wall type for opaque wall (*WWR* = 0), but they were similar to the M wall when the value of the *WWR* increased. It indicated that the influence of insulation is reduced when the value of *WWR* increases for massive wall, and the position of insulation has a small effect on the annual CCL reduction for massive walls.

CHAPTER 5

CONCLUSIONS AND FUTURE RESEARCH

5.1 Conclusions

This research thesis has investigated the effects of the thermal mass on the building envelope, from different directions, various time uses of building, and different *WWR*, using a simulation method and verifying the simulation program with an actual field experiment.

A simulation program, the Building Energy Simulation Program : BESim, was used. The verification of the simulation program showed that it corresponded closely with predicted heat flux on the inner surface of the test wall. The accuracy of the program was statistically analyzed by field measurements. It was found that the root mean square error (RMSE) was 2.547 W/m^2 and the mean bias error (MBE) was + 1.881 W/m^2, which give satisfactory results.

The behavior of heat transfer through thermal mass varied, depending on the thermal mass quantity, orientation and the time use of the air conditioning. It affected considerably on the CCL of the air conditioning. The window to wall ratio, *WWR*, of the building envelope also had an influence on the stored heat of thermal mass of the building envelope.

5.1.1 The Thermal Mass of Opaque Walls

- During the daytime, a large amount of thermal mass resulted in a low cooling load. The east wall has the highest CCL. The north wall has the lowest CCL. The thermal mass from 200 kJ/m^2K to 300 kJ/m^2K were suitable.
- In the daytime and evening, the small amount of thermal mass caused the low CCL. When the thermal mass increased from 20 kJ/m^2K to 120 kJ/m^2K, the CCL also increased. The annual CCL is highest when the thermal mass was between 100 kJ/m^2K - 140 kJ/m^2K. For the south wall, the west wall and the east wall there were slight differences of CCL. The north wall had clearly the lowest CCL. The small amount of thermal mass was suitable for this case.
- At night, the west wall, the south and the east wall gave similar results for the annual CCL. The north wall had the lowest CCL. The small amount of thermal mass was suitable for this case.

- For 24 hours operation, the CCL of the west wall, the south wall and the east were very similar to each other. The north wall has the lowest CCL. The annual CCL decreased when the thermal mass increased. The CCL had a sharp reduction when the thermal mass increased from 20 kJ/m2K to 300 kJ/m2K. The thermal mass from 200 kJ/m^{2}K to 300 kJ/m^{2}K were suitable for this case.

5.1.2 The Effect of *WWR* on Thermal Mass

The simulation results indicate that the CCL reduction rate , by increasing the value of thermal mass, decrease when the value of the *WWR* increases. It can be concluded that thermal mass is less effective in reducing CCL when the value of the *WWR* increases.

5.1.3 The Effect of Insulation Position on the Massive Wall

The insulation is assumed that placed as one layer or two equivalent layers on the outer surface, the inner surface and the mid-center of the brick wall (four wall formations).

Under conditions when there are no windows

- In the daytime, the M wall had the highest CCL. For the insulated walls, the IM wall had the highest CCL, followed by MIM, and MI respectively. The IMI wall was the best wall formation for reducing the CCL.
- In the daytime and evening, the M wall had the highest CCL. For the insulated walls, the MIM wall had the highest CCL, followed by the IM and MI respectively. The IMI wall was the best wall formation for reducing the CCL.
- At night, the M wall had the highest CCL. For the insulated walls, the MIM wall had the highest CCL, followed by the IM and MI, respectively. The IMI wall was the best wall formation for reducing the CCL.
- For 24 hour operations, the M wall had the highest CCL. For the insulated walls, the MI wall had the highest CCL and follow by MIM and IMI respectively. The IM wall was the best wall formation for reducing the CCL.

It may be concluded that the IMI wall is the most suitable for massive wall for reducing the cooling load of buildings.

Under different *WWR* conditions

- In the daytime, The annual CCL increases when the value of *WWR* increases. The annual CCL of the insulated walls are similar to the M wall when the value of *WWR* increases. It indicates that the influence of insulation is reduced when the *WWR* increases for massive wall, and the position of insulation has little effect on the annual CCL reduction for massive walls for this case.
- In the daytime and evening, The annual CCL of the insulated walls are similar to M wall when the value of *WWR* increases. For daytime and evening operations, the influence of insulation is reduced when the *WWR* increases for massive walls, and the position of insulation has little effect on the annual CCL reduction for massive walls.
- At night, the insulated wall with the inner thermal mass causes high CCL because the stored heat of the inner mass is released at night. It may be concluded that the insulated wall with the inner thermal mass is unsuitable for night operated buildings, particularly buildings which have a window area.
- For 24 hour operations, the influence of insulation is reduced when the value of *WWR* for massive wall increase, and the position of insulation has little effect on the annual CCL reduction for massive walls, the same as during the daytime.

5.2 Future Work

- Compare the CCL of the suitable thermal mass with the current building envelope materials.
- Investigate the optimal thermal mass in terms of economy.
- Investigate the balance of the heat resistance and heat capacitance of the building envelope, in order to determine the energy effectiveness.

REFERENCES

Antonopoulos, K.A. (1999), Envelope and indoor thermal capacitance of buildings, *Applied Thermal Engineering*, **19**, pp. 743-756.

Argiriou, A. (1992), *A study of thermal mass in Hellenic building*. Institute for Technological Applications, Hellenic Productivity Centre, Athens.

Baer, S. (1983), 'Raising the open *U* value by passive means', *Proceedings of the 8th National Passive Solar Conference*, pp. 839-842, Glorieta, NM.

Balcomb, J and Jones, R. (1988), *Workbook for Workshop on Advanced Passive Solar Design*. Balcomb Solar Associates, Bled, Yugoslavia.

Balaras, C.A. (1996), The role of thermal mass on the cooling load of building. An overview of computational methods. *Energy and Building*, **24**, pp.1-10.

Balaras, C. (1996), Thermal comfort / Cooling load of buildings / Heat attenuation . *In:* Santamouris,M.and Asimakopoulos,D. 1996. *Passive cooling of buildings.* James & James (Science Pulishers) Ltd, UK.

Bansal, N. K. and Hauser, G. (1994), *Passive building design : a handbook of natural climate control*. Elsevier Science B.V., Amsterdam.

Burch, D., Malcolm, S. and Davis, K. (1984), *ASHRAE Transactions*, Vol. 90, pp. 5-21.

Chirarattananon, S.(2005), *Building for energy efficiency*. AIT, school of environment Resources and development, Thailand

DEDE, (2007), *Standard of energy conservation in building*. Department of Alternative Energy Development and Efficiency, Thailand

Fernandez, J.L., Porta-Gandara, M.A. and Chargoy, N. (2005), Rapid on-site evaluation of thermal comfort through heat capacity in buildings, *Energy and Building*, **37**, pp.1205-1211.

Givoni, B.(1998), Effectiveness of mass and night ventilation in lowering the indoor daytime temperatures : Part I, *Energy and Building*, **28** , pp.25-32.

Gregory, K., Moghtaderi, B., Sugo, H. and Page, A., (2007), Effect of thermal mass on thermal performance of various Australian residential constructions systems, *Energy and building*, Available online : http://www.sciencedirect.com.

Hopkin, V., Gross, G. and Ellifritt, D, (1979). 'Comparing the thermal performances of buildings of high and low masses', *ASHRAE Transactions*, Vol. 85, No. 1, pp. 885-902.

IEA (2006), *Energy Technology Perspective : Scenarios and Strategies to 2050*, OECD/IEA, Paris.

Janda, K.B. and Busch, J.F. (1994), Worldwide status of energy standards for buildings, *Energy-The International Journal*, **19**, 1, pp. 27-44.

Kalogirou, Soteris.A., Florides, G. and Tassou, S.(2002) Energy analysis of buildings employing thermal mass in Cyprus*, Renewable Energy*, 27, pp.353-368

Kontoleon, K.J. Eumorfopoulou, E.A.(2007), The influence of wall orientation and exterior surface solar absorptivity on time lag and decrement factor in the Greek region, *Renewable Energy*, Available online : http://www.sciencedirect.com.

Kosny, J., Petrie, T., Gawin, D., Childs, P., Desjarlais, A. and Christian, J. 2000. *Thermal mass – Energy savings potential in residential buildings*. ORNL, Buildings Technology Center, USA.

Lechner, N.(1991). *Heating, Cooling, Lighting*. John Wiley & Sons, New York.

Ober, D. and Wortman, D., (1991), *ASHRAE J*., **33**, pp. 18-21.

Ogoli, D.M. (2003), Predicting indoor temperatures in closed buildings with high thermal mass, *Energy and Building*, **35**, pp.851-862.

Petcharat, S. (2002), *Effect of shading on heat transfer through opaque wall*. School of Energy and Materials, KMUTT, Thailand.

Saman, N. and Fazzolari, R. (1991), Prediction of preconditioning and storage loads after system shutdown using DOE-2, *ASHRAE Transactions*, 97, 1, pp. 320-324.